Interaction in the systems of fluid–melt–crystal

Chevychelov V.Y., Plyusnina O.E., Viryus A.A. On the solubility of fluorides in melt of natural potassium syenite UDC 550.42

D.S. Korzhinskii Institute of Experimental Mineralogy of Russian Academy of Sciences (IEM RAS)
(chev@iem.ac.ru, o_plusnina@mail.ru, mukhanova@iem.ac.ru)

Abstract. The solubility of fluorides in a fluid-saturated melt of natural potassium syenite from the Tabornoe gold deposit at *T* = 900-600°C, *P* = 250-150 MPa has been experimentally investigated. The experiments were carried out to confirm the hypothesis of a sufficiently high solubility of fluorine in the melt of ultrapotassium syenites, which could contribute to the formation of specific and low-viscosity melts embedded in the form of sills. The chemical composition of the syenite used in the experiments (in wt.%): SiO_2 - 63.9, TiO_2 - 0.2, Al_2O_3 - 16.8, Fe_2O_3 - 2.0, MnO - 0.1, MgO - 0.1, CaO - 1.0, Na_2O - 0.2, K_2O - 15.8, PPP - 2.5, Σ - 97.3.

As a result of the experiments, the acidity-alkalinity of the fluid coexisting with the melt sharply changed: the acidic initial solution (pH = 2-2.5) became alkaline (pH = 9). The temperatures of solidus (613 ± 13°C) and liquidus (725 ± 75°C) of the studied melt were determined. According to the data of the wave X-ray spectrometer, rather high fluorine contents in the syenite melt were obtained, up to 4.0-4.2 wt.% F in the range 650-800°C and up to 4.0-5.0 wt.% F at 625°C.

Keywords: *solubility, fluoride, experiment, potassium syenite, melt, solidus, liquidus*

The solubility of fluorides in a fluid-saturated melt of natural potassium syenite from the Tabornoye gold deposit (northwest of the Aldan shield) at *T* = 900 – 600 °C, *P* = 250 -150 MPa has been experimentally investigated. The experiments were carried out to confirm the hypothesis of a sufficiently high solubility of fluorine in the melt of ultrapotassic syenites, which could contribute to the formation of specific and low-viscosity melts embedded in the form of sills. Early Cretaceous syenite sills of the second phase were introduced after the manifestation of metasomatism and the formation of gold mineralization, but close in time to these events (Zubkov et al., 2020). For this reason, as well as due to the presence of a common potassium specificity for metasomatic transformations and syenites, their paragenetic connection is assumed. According to petrographic data, syenites correspond to igneous rocks; however, in terms of the content of petrogenic elements, they are quite close to the monomineral melt of the composition of K-feldspar. The chemical composition of potassium syenite used in the experiments (wt.%): SiO_2 - 63.9, TiO_2 - 0.2, Al_2O_3 - 16.8, Fe_2O_3 - 2.0, MnO - 0.1, MgO - 0.1, CaO - 1.0, Na_2O - 0.2, K_2O - 15.8, PPP - 2.5, Σ - 97.3.

The task of our experiments was to determine the solubility of fluorine in the ultrapotassium syenite melt, as well as to determine the solidus temperature of this melt at the maximum contents of fluorine and water in the melt. The experiments were carried out in double platinum capsules. In this case, a mixture of potassium syenite powder (22.5 mg) and hieratite K_2SiF_6 (7.5 mg), as well as an aqueous solution of 1n HF + 1n KF (6 mg) were placed inside a small capsule (outer diameter 4 mm, wall thickness 0.2 mm, length 18-20 mm). Then, a small capsule was sealed and placed inside a large capsule (7 mm × 0.2 mm × 25–35 mm). The calculated amount of distilled water was poured into a large capsule taking into account the *P-V-T* coefficient of water at conditions of the experiment. Then the capsule was sealed. The experiments were carried out in an internally heated pressure vessel (IHPV). Each experiment was first heated to *T* = 850°C at *P* = 250 MPa and held for 5-6 hours to obtain a homogeneous melt. Then the *T-P* parameters of the experiment were reduced and the experiment was continued at 800°C, 250 MPa; at 650°C, 150 MPa or at 600°C, 150 MPa for about 7-8 days (Table 1). To clarify the solidus temperature, one experiment was carried out without preliminary melting of the charge at 625°C, 150 MPa for about 8 days. The experiments were quenched isobarically. The temperature drop rate was up to 70-80 deg/min. The solid products of the experiments were analyzed by the method of X-ray spectral microanalysis using energy-dispersive (for the main petrogenic elements) and crystal-diffraction (for fluorine) spectrometers.

Table 1. Initial data of experiments and obtained results.

Run number	Rock sample number, (Ca, wt.%)	*T* melting, °C	*T* run, °C	*P*, kbar	Duration, day	F in glass*, wt.%	End products of run, wt.%
OP-2a	1 (1.33)	850	800	≈2.5	0.2+7.8	3.3-4.2	aluminosilicate glass (40), pores (45), fluoride phase (15)
OP-3a	1 (1.33)	800	650	≈1.5	0.2+6.8	2.3-4.1	aluminosilicate glass

Run number	Rock sample number, (Ca, wt.%)	*T* melting, °C	*T* run, °C	*P*, kbar	Duration, day	F in glass*, wt.%	End products of run, wt.%
							(38), pores (40), fluoride phases (17), potassium feldspar (5)
OP-3b	2 (0.96)	800	650	≈1.5	0.2+6.8	2.7-3.8	aluminosilicate glass (40), pores (32), fluoride phases (20), potassium feldspar (8)
OP-4a	1 (1.33)	800	600	≈1.5	0.3+7.0	No glass	potassium feldspar (75), quartz (13), fluoride phases (7), fluorite (5)
OP-4b	1 (1.33)	There was no premelting	625	≈1.5	7.6	2.3-4.9	potassium feldspar (65), fluoride phases (15), aluminosilicate glass (13), fluorite (7)

* Wave spectrometer

Table 2. End products of run. Compositions of aluminosilicate glass and potassium feldspar (wt.%)*

	SiO_2	TiO_2	Al_2O_3	Fe_2O_3	CaO	Na_2O	K_2O	F	Σ
Aluminosilicate glass	64.7	0.2	11.7	1.9	0.1	0.1	11.6	3.5	94.0
Potassium feldspar	62.6	-	16.7	1.4	-	-	17.2	-	99.9

* EDS spectrometer

Table 3. End products of run. Compositions of fluoride phases and fluorite (at.%)*

	Al	Mg	Ca	Na	K	F	Σ
K_3AlF_5 - fluoride phase	11.0	-	0.3	0.5	34.6	53.1	99.9
$K_2Mg_2F_5$ - fluoride phase	0.2	20.3	0.6	0.2	24.4	53.4	99.9
Fluorite	-	-	40.2	0.1	0.5	58.4	100

* EDS spectrometer

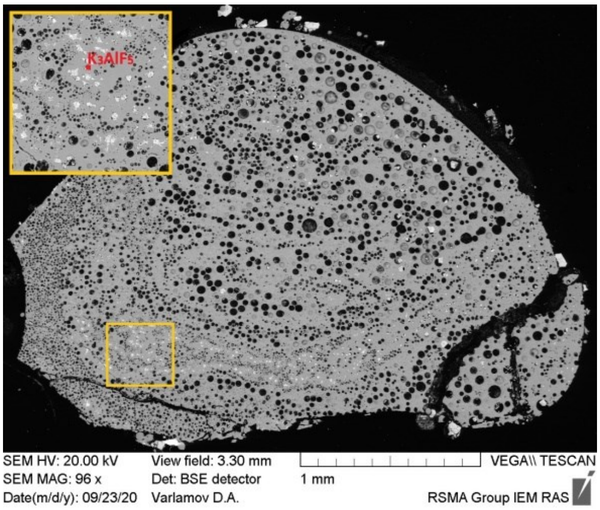

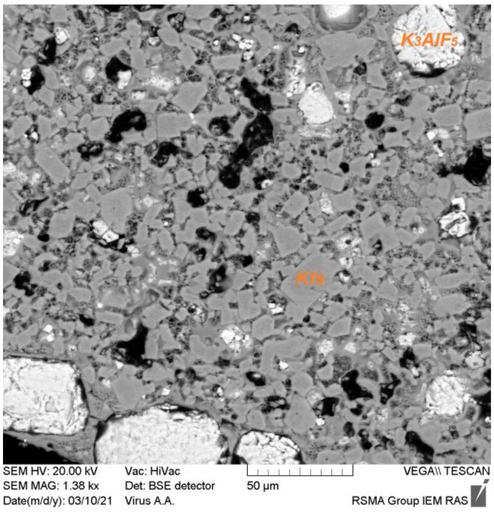

Fig. 1. Nonuniform partitioning of porosity and fluorides in glasses. Backscattered electron image (BSE).
Fig. 2. The initial melting of the rock sample takes place. Experiment OP-4-b, T= 625°C, P= 1.5 kbar. Backscattered electron image (BSE).

After the experiments, the obtained experimental products contained aluminosilicate glass, potassium feldspar, quartz, as well as K_3AlF_5 and $K_2Mg_2F_5$ fluoride phases and fluorite. Table 1 shows the quantitative ratios of these phases after the experiments, estimated from photographs of polished sections. The compositions of the individual phases are given in Tables 2 and 3. The higher-temperature samples were characterized by high porosity, they contained up to 30-45 % pores. As a result of the experiments, the acidity-alkalinity of the fluid coexisting with the melt sharply changed: the acidic initial solution 1n HF + 1n KF (pH = 2-2.5) became alkaline (pH = 9). This is due to the dissolution of HF in the melt and the removal of potassium from the melt into the fluid.

According to the results of a series of experiments at various *P-T* conditions, it was found that two phases coexist at temperatures above 800°C: aluminosilicate melt and fluoride phase close in stoichiometry to potassium fluoroaluminate K_3AlF_5, the distribution of which in the sample is often nonuniformly (Fig. 1). At the temperature drops to 650°C, idiomorphic grains of potassium feldspar (5-8 % by volume) begin to crystallize from the melt. At temperature of 600°C, the melt is completely crystallized forming an association: K-feldspar (75 %), quartz (13 %), fluoride phase (7 %), fluorite (5 %). At $T = 625^oC$, $P = 150$ MPa, in the experiment without preliminary melting of the charge, the initial melting of the sample was obtained (experiment OP-4-b, Fig. 2). The products contain about 13 % of the melt (Fig. 2, Table 1) in association with K-feldspar (65 %), fluoride phases (15 %) and fluorite (7 %).

The temperatures of solidus (613 ± 13°C) and liquidus (725 ± 75°C) of the studied melt were determined. Rather high fluorine contents in the melt of alkaline potassium syenite were obtained: up to 4.0-4.2 wt.% in the range 650 -800°C and up to 4.0-5.0 wt.% at 625°C (Table 1).

Conclusions

1. The strong alkalinity of an aqueous fluoride fluid coexisting in equilibrium with ultrapotassium syenite melt has been established.
2. The temperatures of solidus (613 ± 13°C) and liquidus (725 ± 75°C) of the studied syenite melt saturated with fluid and fluorine have been estimated.
3. High solubility of fluorine in fluid-saturated ultrapotassium syenite melt was determined (up to 4.0-4.2 wt.% in the range 650 -800°C, $P = 150$-250 MPa and up to 4.0-5.0 wt.% at 625°C, $P = 150$ MPa).
4. The initial crystallization of potassium feldspar grains from the melt in a series of experiments coincides with that observed in natural samples.

Acknowledgments. The authors are grateful to A.R. Kotelnikov for help and advice in the work.

References

Zubkov Yu.A., Sagir A.V., Chvarova N.V. "Uguisky" type of large-volume gold deposits formed in the linear weathering crust (southwestern Yakutia) // Otechestvennaya geologiya. - 2020. - No. 2. - P. 32-45. (in Russian)

Chevychelov[*1] V.Y., Kotelnikov[1] A.R., Peretyazhko[2] I.S., Viryus[1] A.A., Suk[1] N.I., Savina[2] E.A. Low-pressure high-temperature melting of marly limestone from the pyrometamorphic complex of Mongolia (first results) UDC 550.42

[1] D.S. Korzhinskii Institute of Experimental Mineralogy of Russian Academy of Sciences (IEM RAS); [2] A.P. Vinogradov Institute of Geochemistry of SB RAS
(chev@iem.ac.ru*, kotelnik1950@yandex.ru, pgmigor@mail.ru, mukhanova@iem.ac.ru, sukni@iem.ac.ru)

Abstract. The experiments were carried out at $T = 1300^oC$, $P = 10$-12 MPa, and an increased partial pressure of CO_2. Our task was to determine the conditions for the formation of melilite-nepheline paralava and carbonate melt formed as a result of the melting of limestone containing 40 wt.% of pelitic material. Chemical composition of the rock used in the experiments (wt.%): 16.3 SiO_2, 0.3 TiO_2, 9.1 Al_2O_3, 0.8 Fe_2O_3, 0.4 FeO, 0.1 MnO, 1.9 MgO, 39.9 CaO, 2.6 Na_2O, 0.3 K_2O, 0.2 P_2O_5, 26.2 CO_2, 1.5 H_2O^+, 0.5 H_2O^-, 0.2 S_{tot}, 0.2 SrO, 100.6 Σ.

The first results show the presence of the following phases in the run products (microprobe analysis, wt.%): (?) larnite Ca_2SiO_4 - 64.1-65.0 CaO, 25.5-31.4 SiO_2, 1.8-2.8 Na_2O, 0.7-2.0 MgO, 0.3-1.1 TiO_2, 96.8 -101.3 Σ; (?) helenite $Ca_2Al_2SiO_7$ - 43.2-45.2 CaO, 35.5-40.6 Al_2O_3, 14.5-19.6 SiO_2, 0.5-1.1 MgO, 99.6-103.2 Σ; calcite $Ca(CO_3)$ - 57.8-58.2 CaO, 0.4-0.6 SrO, 60.0-61.5 Σ and quench products of two melts: alkaline-carbonate - 33.9-34.8 CaO, 11.6-12.2 Na_2O, 3.7-3.9 K_2O, 1.8-4.1 SO_3, 53.4-56.0 Σ and carbonate-silicate - 43.3-48.4 CaO, 13.7-14.9 SiO_2, 9.4-10.9 Al_2O_3, 2.6-3.6 Na_2O, 2.3-2.9 MgO, 0.4-0.8 TiO_2, 0.3-0.6 K_2O, 0-0.8 SrO, 73.6 -83.0 Σ. The phases similar in composition were obtained in the experiment without increased CO_2 pressure, excluding the carbonate-silicate melt.

Keywords: *low-pressure, high-temperature, experiment, melting, marly limestone, melilite-nepheline paralava, carbonate melt, pelitic material*

The results of low-pressure high-temperature experiments on melting marly limestone from the Khamaryn-Khural-Khiid pyrometamorphic complex at $T = 1300^oC$, $P = 10$-12 MPa are presented. Such complexes in Mongolia were formed during pyrogenic metamorphism and partial melting of carbonate-silicate sedimentary rocks caused by natural underground coal fires (Peretyazhko et al., 2017; Peretyazhko et al., 2018; Savina et al., 2020; Peretyazhko et al., 2021). The task of our experimental studies was to determine the conditions for the formation of melilite-nepheline paralava and carbonate melt, which are formed as a result of incongruent melting of marly limestone containing about 40 wt.% of pelitic material. The chemical composition of the MN-1423 carbonate-silicate rock used in the experiments is as follows (relict of marly limestone, wt.%): 16.3 SiO_2, 0.3 TiO_2, 9.1 Al_2O_3, 0.8 Fe_2O_3, 0.4 FeO, 0.1 MnO, 1.9 MgO, 39.9 CaO, 2.6

Na_2O, 0.3 K_2O, 0.2 P_2O_5, 26.2 CO_2, 1.5 H_2O^+, 0.5 H_2O^-, 0.2 S_{tot}, 0.2 SrO, 100.6 Σ.

The experiments were carried out in platinum capsules. A powder of the studied carbonate-silicate rock (20-50 mg) was placed in one small capsule with an outer diameter of 4 mm, a wall thickness of 0.2 mm and a length of 18-20 mm, and freshly prepared silver oxalate $Ag_2C_2O_4$ (30-40 mg), which was synthesized by the reaction $2AgNO_3 + Na_2C_2O_4 \rightarrow Ag_2C_2O_4\downarrow + NaNO_3$ by merging salt solutions and drying the precipitate, was loaded into same another small capsule. After that, both small capsules were compressed 2/3 of their length, but they were not sealed and placed inside a large capsule (10 mm × 0.2 mm × 50 mm), which then was sealed. The assembled construction of three capsules was kept at 120-130°C for 2-4 hours to decompose silver oxalate by the reaction $Ag_2C_2O_4 \rightarrow 2Ag + 2CO_2\uparrow$. The experiments were carried out on an internally heated pressure vessel (IHPV), in which the pressure inside the capsule was equalized with the external pressure on the capsule, that was established using an inert gas argon. For comparison, an experiment was also carried out without silver oxalate (i.e. without the initially increased partial pressure of CO_2 in the system). The duration of the experiments was 6 hours. The quenching conditions were close to isochoric (simultaneous decrease in temperature and pressure).

After the experiment, the large capsule was "expanded". The experiment was opened as follows: (1) the capsule was weighed, then the capsule was frozen in liquid nitrogen for 3 min, then several holes were pierced in the capsule and kept for 3 min in air to heat up to room temperature, while the excess of gas phase (mainly CO_2) was removed from the capsule through the holes, the capsule was weighed, (2) then the capsule was heated at 100°C for 3 minutes, while the liquid phase was removed from the capsule through holes, then the capsule was kept in air for 3 minutes to cool to room temperature and weighed. At the opening of PRT-2b experiment, 15.5 mg of the gas phase and less than 0.5 mg of the liquid phase were released from the capsule. It can be assumed that 11.5 mg of the gas phase was preliminarily formed due to the decomposition of silver oxalate at a low temperature of 120-130°C, and the remaining 4 mg were formed in the experiment at a high temperature due to the decomposition of calcite from the studied rock. When examined sample with a binocular microscope after the experiment, the carbonate-silicate rock was an aggregate of whitish grains and their fragments with varying degrees of transparency and homogeneity. These obtained solids were press-fit into polystyrene and then analyzed by X-ray spectral microanalysis using EDS.

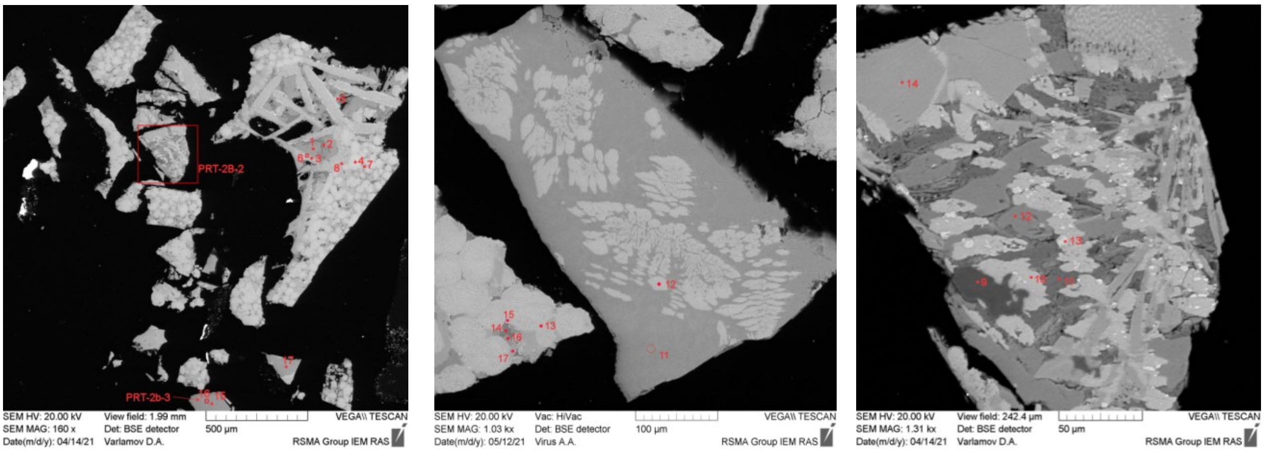

a b c

Fig. 1a, 1b, 1c. End products of PRT-2b experiment, system with $Ag_2C_2O_4$, P_{CO2} ≈11.6 MPa, T = 1300°C, P_{tot} = 12.5 MPa, duration 6 hours. Backscattered electron image (BSE).

The following phases were defined in the end products of the experiment:

(?) <u>larnite</u> Ca_2SiO_4 (wt.%) - 62.0-65.6 CaO, 22.3-31.4 SiO_2, 1.8-3.3 Na_2O, 0.7-2.0 MgO, 0-2.4 Al_2O_3, 0-1.1 TiO_2, 91.3-101.2 Σ. Blond round (spherical) formations. Quenching crystallization (elongated, needle-like crystals) is often visible in them. Separate prismatic and elongated crystals are also distinguished (Fig. 1a. 4; Fig. 1b. 12, 13; Fig. 1c. 10).

(?) <u>helenite</u> $Ca_2Al_2SiO_7$ (wt.%) - 43.2-45.2 CaO, 35.5-40.6 Al_2O_3, 14.5-19.6 SiO_2, 0-1.1 MgO, 98.8-103.2 Σ. Gray, darker than larnite, phase accommodating larnite. Gelenite also forms elongated, tabulated and skeletal dendritic crystals (Fig. 1a. 3, 7, 8; Fig. 1b. 17; Fig. 1c. 14).

<u>calcite</u> $Ca(CO_3)$ <u>or quenching products of calcite melt</u> (wt.%) - 57.6-58.2 CaO, 0.5-0.6 SrO, 58.3-61.5 Σ, + CO_2. A blonder phase in comparison with the alkaline-carbonate melt (Fig. 1a. 1; Fig. 1c. 12).

<u>quenching products of the alkali-carbonate melt</u> (wt.%) - 33.8-34.8 CaO, 11.6-12.3 Na_2O, 3.7-4.3 K_2O, 1.7-4.1 SO_3, 0-0.6 SrO, 52.4-56.0 Σ, + CO_2.

Visually darker phase compared to calcite (Fig. 1a. 2; Fig. 1b. 14; Fig. 1c. 11).

periclase MgO (wt.%) - 74.9 MgO, 10.9 Al_2O_3, 2.6 CaO, 1.3 TiO_2, 1.0 SiO_2, 0.5 Cr_2O_3, 92.7 Σ. The darkest phase in the sample (Fig. 1c. 9).

phase Ca-Ti-Si-Al-O (wt.%) - 44.8-52.9 CaO, 26.0-42.6 TiO_2, 6.6-13.0 SiO_2, 1.6-3.6 Al_2O_3, 1.8-2.9 MgO, 1.5-2.8 PtO_2 (ZrO_2), 0.6 -1.8 Na_2O, 0-0.5 K_2O, 99.2-105.3 Σ. The brightest and lightest phase in the sample (Fig. 1a. 5; Fig. 1b. 15; Fig. 1c. 13).

quenching carbonate-silicate glass, fig. 2 (wt.%) - 43.3-48.4 CaO, 13.7-14.9 SiO_2, 9.4-10.9 Al_2O_3, 2.6-3.6 Na_2O, 2.2-2.9 MgO, 0.4-1.1 TiO_2, 0.3-0.6 K_2O, 73.6-83.0 Σ, + CO_2. This phase was segregated in the form of separate flat grains, absolutely transparent and homogeneous in appearance (Fig. 1a. 15, 16, 17). The compositions of different grains can differ in the SiO_2/Al_2O_3 ratio.

In the experiment without silver oxalate and at $P_{tot} \approx 10$ MPa, the phases similar in composition were obtained, excluding the carbonate-silicate glass.

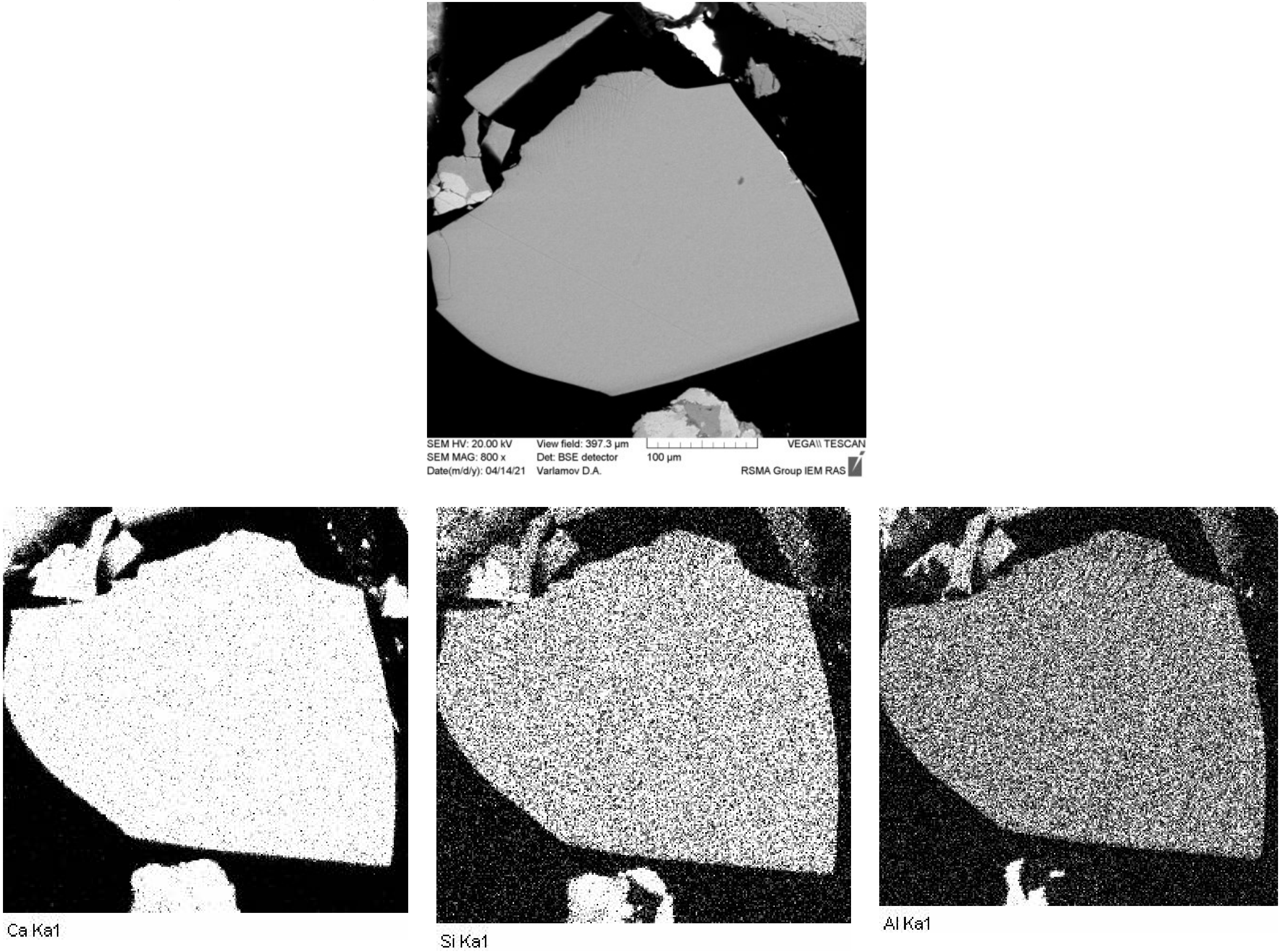

Fig. 2. Quenching carbonate-silicate glass. Backscattered electron imaging (BSE) and area mapping (CaKα_1, SiKα_1, AlKα_1). End products of PRT-2b experiment.

References

Peretyazhko I.S., Savina E.A., Khromova E.A. Low-pressure (> 4 MPa) and high-temperature (> 1250°C) incongruent melting of marly limestone: formation of carbonate melt and melilite-nepheline paralava in the Khramaryn-Khural-Khiid combustion metamorphic complex, East Mongolia // Contributions to Mineralogy and Petrology. - 2021. - V. 176, No 5. - P. 28.

Peretyazhko I.S., Savina E.A., Khromova E.A. Minerals of the rhonite-kuratite series in paralavas from a new combustion metamorphic complexes in the Choir-Nyalga basin (Central Mongolia): composition, mineral assemblages and formation conditions // Mineralogical Magazine. - 2017. - V. 81, No 4. - P. 949-974.

Peretyazhko I.S., Savina E.A., Khromova E.A., Karmanov N.S., Ivanov A.V. Unique clinkers and paralavas of the new Nyalga pyrometamorphic complex in Central Mongolia: mineralogical and geochemical features, conditions of formation // Petrology. - 2018. - Vol. 26, No. 2. - P. 178-210. (in Russian)

Savina E.A., Peretyazhko I.S., Khromova E.A., Glushkova V.E. Melted rocks (clinkers and paralavas) of the Khramaryn-Khural-Khiid pyrometamorphic complex, Eastern Mongolia: mineralogy, geochemistry, formation processes // Petrology. - 2020. - Vol. 28, No. 5. - P. 482-510. (in Russian)

Lebedev E.B. Influence of volatile components on the evolution of the biosphere

GEOHI RAS

Abstract Water stands apart in the history of our planet. There is no natural body that could compare with it in terms of its influence on the course of the most grandiose geological processes and the origin of the biosphere. V. I. Vernadsky wrote in the History of Natural Waters that water, the main volatile component contained in magmas, far exceeds other components in quantity and significantly affects the changes in the chemical and physical properties of rocks and melts. E. M. Galimov pointed out that the primary environment on Earth contained water minerals, H_2O, CO_2, CO, CH_4, NH_3, and water always stood out in the first place.

The water content in various layers of the Earth's crust was estimated by many researchers, but their approach allowed us to judge only the presence of bound water in the rocks and did not indicate the content of free water. Experimental studies have made it possible to determine the water content in the rocks of the Earth's crust and upper mantle – in melts of albite, granite, basalt, to study the solubility, viscosity, electrical conductivity, elastic wave velocity and other physico-chemical properties of rock melts under water pressure. Experimental studies have shown that water and various solutions strongly affect the physical and chemical properties of melts and rocks as a result of mineral reactions and changes in the structure of magmatic melts and rocks. The obtained results of the study of the role of volatile components in geochemical and geophysical processes will contribute to the deepening of the petrophysical and geochemical interpretation of geophysical observations, as well as the problems of the evolution of the biosphere.

Keywords: *water, the main volatile component, water albite, granite, basalt, physical and chemical properties of rock melts, viscosity, electrical conductivity, elastic wave velocity*

Water stands apart in the history of our planet. There is no natural body that could compare with it in terms of its influence on the course of the most grandiose geological processes and the origin of the biosphere.

V. I. Vernadsky wrote in the "History of Natural Waters" that water is the main volatile component contained in magmas, far surpasses other components in quantity and significantly affects the changes in the chemical and physical properties of rocks and melts (Vernadsky, 1936).

The director and founder of our Institute of GEOCHI RAS of the Russian Academy of Sciences, Academician A. P. Vinogradov, invited N. I. Khitarov, who was engaged in experimental work with autoclaves in Leningrad, to the Institute.

N. I. Khitarov created an experimental laboratory at the Institute, which at first was called Laboratory of magmatogenic processes, now called the Laboratory of Geochemistry of the Earth's Mantle.

One of the main tasks was to study the influence of water on the physico-chemical properties of geological rocks and magmatic melts at high pressures and high temperatures.

N. I. Khitarov organized the first meeting "on esperimental mineralogy, petrology and geochemistry" , which is now called "Khitariada" (Kadik, Lebedev, Khitarov, 1971).

In the monograph "Problems of the origin and evolution of the Biosphere" (Galimov, 2008) in the section "What is life" on the scheme of the Initial stage of the evolution of life, it was indicated that the primary environment on Earth contained minerals, H_2O, CO_2, CO, CH_4, NH_3. Water has always stood out in the first place.

In the book "Fluids in the Earth's Crust", Kissin (2009) provides literary data on the water content in various layers of the Earth's crust. In the Earth's crust, the amount of water up to a depth of 20 km is not less than 8%, without reducing the amount of water up to 60 km (Vernadsky, 1936).

In more recent studies, the amount of water in the " granite "layer is 0.5-1.5%, in the" basalt " layer - 0.1-0.7%, (Gavrilenko, Dorpholz, 1971). The average water content in the rocks of the subsurface layer of the upper mantle and the lower part of the Earth's crust is 0.3-0.5%. This approach allows us to judge only the presence of bound water in the rocks and does not indicate the content of free water (Kissin, 2009).

Many works have been devoted to the experimental study of the water content at high pressures and high temperatures in the rocks of the Earth's crust and upper mantle.

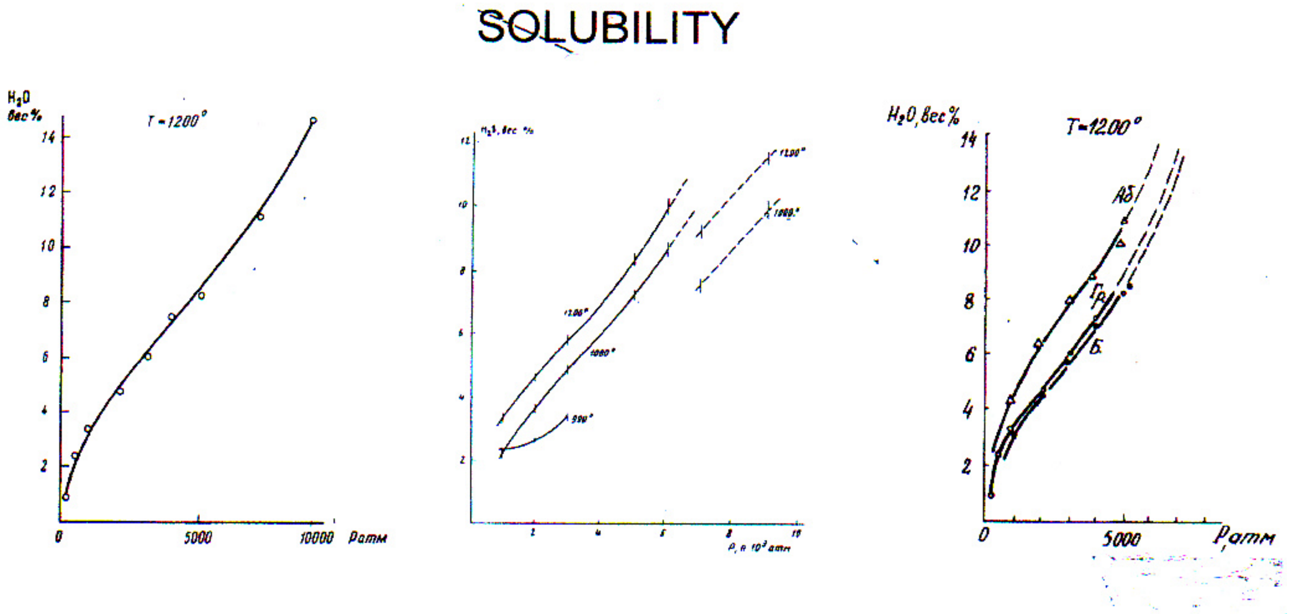

Water solubility in granite melt,

T =1200°C

Water solubility in basalt melt

Water solubility granitie and basalt m

T=1200°C.

Fig. 1. Solubility of water in melts of albite, granite and basalt, at P, etc.

The main result of the experimental data. It is determined how much water can contain and dissolve magmatic melts at high T and R (Kadik, Lebedev, Khitarov, 1971).

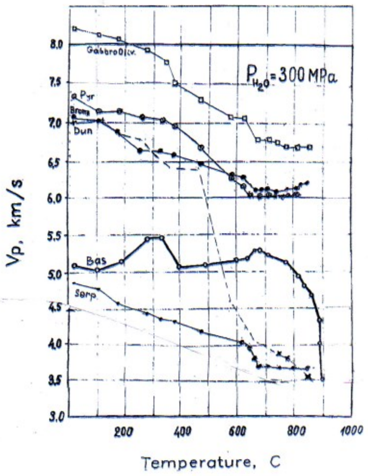

Fig.2

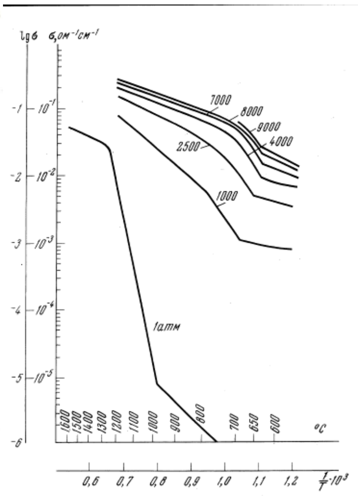

Fig.3

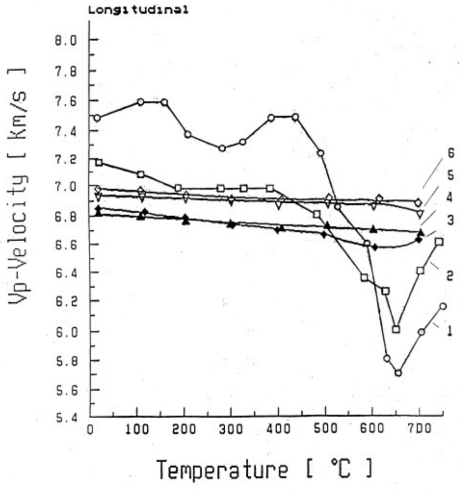

Fig.4

Fig.2. Velocity of elastic waves of rocks under water pressure, at high P and T. Comparison of experimental data obtained in rocks with water at high P and T, and natural, allows you to solve the physicochemical conditions of the ongoing deep processes.

Fig. 3. Electrical conductivity of granite under water pressure, at high P and T (Lebedev, Khitarov, 1964). The study and comparison of the water content in rocks and melts with electrical conductivity allows us to determine the water content in rocks at great depths.

Fig. 4. The speed of elastic waves of amphibolite in dry conditions (straight lines), fractures (under water pressure). A comparison of experimental data obtained under dry conditions and under water pressure shows a sharp difference associated with the course of chemical reactions in amphibolite in the presence of water (Lebedev, Dorfman, Zebrin, 1991).

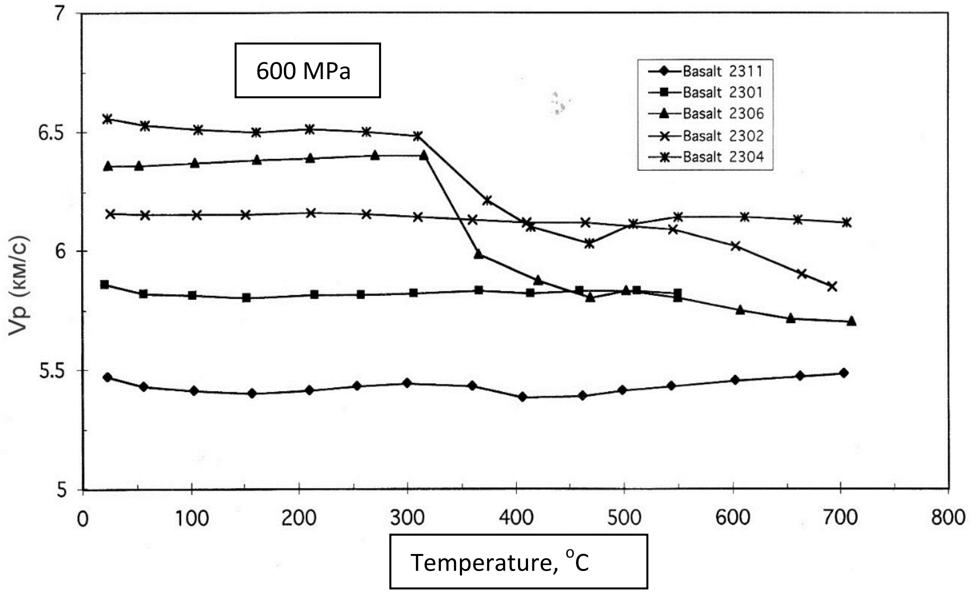

Fig. 5. Karer basalts, water release at T=300°C and P = 600 MPa. Even in dry conditions, up to T=300 °C contain water (Lebedev, Kern, 1999).

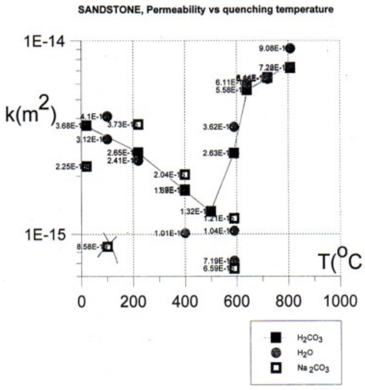

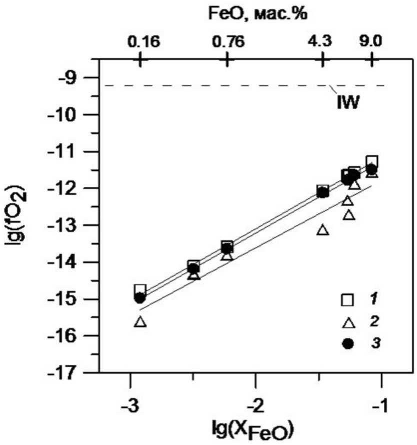

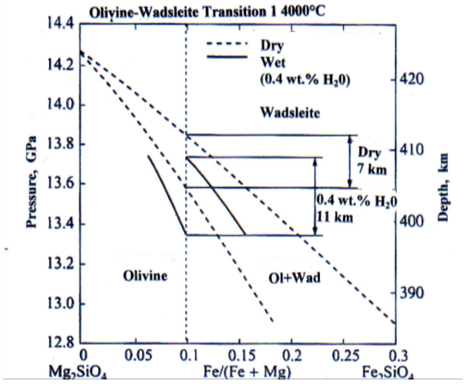

Fig. 6. Sandstone, permeability of a hardened sample with fluids, at P, etc. The permeability of sandstone depends on the microcrackage. It differs for different fluids: H_2O, H_2CO_3, Na_2CO_3 (Zharikov et al., 2000) .

Fig. 7. Oxygen volatility during iron deposition lg f O2 = - 15, T=1400°C. The study of the formation of the Moon's core (Lebedev, Lukanin, 2019). Perhaps a little wte-21ol. 25, No. 2, pp. 21r

Fig.8. Wadsley (Mao et al., 2011), Deeper Setting. At a depth of 300-400 km, olivine turns into wadsleyite, which contains 0.4 wt% H_2O. This is a large amount of water in the whole wadsleyite layer (Mao et al., 2011).

We have determined the water content in the melts of albite, granite, basalt. The physicochemical properties of rock melts under water pressure were studied: solubility, viscosity, electrical conductivity, elastic wave velocity, and others in melts. The drilling depth is 12.5 km, therefore, to represent the water content at great depths, it is necessary to study and compare the water content in rocks and melts with the electrical conductivity and wave velocity during experiments at high pressures and temperatures.

A lot of research has been done on this topic, here are some of them.

Discussion

Experimental studies of the physicochemical properties of various rocks (velocity of elastic properties, edectroconductivity, density, permeability, and arcing) were performed at high pressures both under water pressure and under dry conditions (Galimov, 2008; Kadik et al., 1971; Gavrilenko, Derpgolts, 1971; Kissin, 2009; Krainov et al., 2012).

Systematic measurements were carried out in amphibolites and the dependences of Vp and Vs on pressure and temperature were obtained both in "dry" conditions and under water pressure. The obtained values of Vp and Vs under water pressure differ significantly from similar data for " dry " conditions.

In amphibolite, at the site of velocity reduction (up to 650°C), the process of opening microcracks associated with: the penetration of water as a surfactant into the intergranular space and its possible wedging action (Zharikov et al., 2000); the possible effect of thermal dilatation caused by differences in the coefficients of thermal expansion of minerals; partial dehydration of amphibol, as well as the α-β transition in quartz, can play a decisive role.

The sharpest and most significant decrease occurs during the serpentinization of dunite, which may correspond to a decrease in velocity in the region of reduced velocities in the lithosphere (70-100 km). Pyroxenes during amphibolization affect to a lesser extent.

The triple system MgO — FeO — SiO_2 (Bowen, Tuttle, 1949) is also of interest, in which magnesia-ferruginous olivines crystallize from liquids with very wide limits of composition fluctuations. For some compositions of this system, olivine begins to crystallize first, sharply fractionating, followed by only monoclinic pyroxene for a while, and then there is a joint precipitation of monoclinic pyroxene and olivine again. This latter is much richer in iron than olivine of the first stage of crystallization.

A huge "reservoir" of water, three times the volume of all the oceans of the Earth, has been discovered deep below the Earth's surface. Water is not in a liquid state.

It is enclosed inside the ringwoodite mineral, which is located at a depth of 700 kilometers in the mantle in a layer of hot rocks between the Earth's surface and its core.

Ringwoodite and wadsleite form the surface layer of the Earth's mantle, which has a remarkable ability to absorb water. Ringwoodite can be formed exclusively under extremely high pressure conditions, for example, in the bowels of the earth (525-660 km depth) (Mao et al., 2011).

Conclusion Experimental studies have shown that water and various solutions strongly affect the physical and chemical properties of melts and rocks as a result of mineral reactions and changes in the structure of magmatic melts and rocks.

Acidic, neutral and alkaline fluids have a significant and different effect on the physicochemical properties (seismic, electrical, etc.) of rocks and melts.

The obtained results of the study of the role of volatile components in geochemical and geophysical processes will contribute to the deepening of the petrophysical and geochemical interpretation of geophysical observations, as well as the problems of the evolution of the biosphere.

Below is a list of works related to studies of the water content in melts (Vernadsky, 1936; Galimov, 2008; Kadik et al., 1971; Gavrilenko, Derpgolts, 1971; Kissin, 2009; Krainov et al., 2012; Khitarov et al., 1976; Bowen, Tuttle, 1949; Burnham, Davis, 1971; Lebedev et al., 1991; Lebedev, Kern, 1999; Zharikov et al., 2000) and the influence of water on the physico-chemical properties of rocks and melts (Lebedev, Khitarov, 1964; Kadik et al., 1989; Lebedev, Lukanin, 2019; Khitarov et al., 1976; Zharikov et al., 2000; Mao et al., 2011).

References

Bowen N. L., Tuttle O. F. The system MgO-SiO_2-H_2O. Geol. Soc. Amer. Bull., 1949, v. 60. p. 439-460.

Burnham C.W., Davis N.F.. The role of H_2O in silicate melts P-V-T relations in the system $NaAlSi_3O_8$-H_2O to 10 kilobars and 1000°C. 1971. The Pennsylvania State University.

Galimov E. M. Problems of the origin and evolution of the biosphere. (Edited by E. M. Galimov). M. 2008. 552.

Gavrilenko E.S., Derpgolts V.F., 1971. Hydrosphere of the Earth. Kiev: Naukova Dumka, 272 p.(in Russian)

Kadik A. A., Lebedev E. B., Khitarov N. I., 1971. Water in magmatic melts. M., "Science", 254 p.

Kadik A. A., Zebrin S. R., Dorfman A.M., 1989. Experimental study of the influence of water on the velocity of elastic waves of deep rocks. DAN USSR, volume 309, N 5, 1090-1093).

Khitarov N. I., Lebedev E. B., Dorfman A.M., 1976. Physical properties of the silica-water system at high parameters. Geochemistry, 2, 217-222 .

Kissin I. G. Fluids in the Earth's Crust" (2009). Nauka, Moscow, 328 p.

Krainov S. R., Ryzhenko B. N., Shvets V. M. Geo-chemistry of underground waters. Theoretical, applied and environmental aspects. M. TSLNG 2012, 672 p.

Lebedev E. B., Khitarov N. I., 1964. The beginning of the melting of granite and the electrical conductivity of its melt, depending on the high pressure. Geochemistry, 3, 195-201.

Lebedev E. B., Lukanin O. A. 2019 18 Interd. Conf. FHPFSZ Oxygen volatility during iron deposition lg f O_2 = - 15, T=1400°C. The study of the formation of the Moon's core.

Lebedev E.B., Dorfman A.M., Zebrin S.R., 1991. Study of the mechanism of the influence of water on elastic wave propagation in amphibolites and some metamorphic rocks at high pressures and temperatures. Phys. Earth Planet. Inter., 66, 313-319)

Lebedev E.B., Kern H. The effect of hydration and dehydration reactions on wave velocities in basalts. Tectonophysics, 1999, 308,

Mao Z., Jacobsen S.D., Frost D.J., McCammon C.A., Hauri E.H. , and Duffy T.S. Effect of hydration on the single-crystal elasticity of Fe-bearing wadsleyite to 12 GPa Amer. Mineral, 2011.V. 96. P.1606-1612,

Vernadsky V.I. The History of natural waters. 1936.

Zharikov A. V., Lebedev E.B., Dorfman A.M., Vitovtova V.M., 2000. Effect of Saturating Fluid Composition on the Rock Microstructure, Porosity, Permeability and Vp under High Pressure and Temperature. Phys. Chem. Earth (A).

Persikov E.S., Aranovich L.Ya, Bukhtiyarov P.G., Nekrasov A.N., Bondarenko G.V.

Experimental modeling of the iron carbide (Fe_3C) interaction process with hydrogen at temperatures of 1000-1150^oC and pressures of 30-100 MPa

IEM RAS. Chernogolovka. (persikov@iem.ac.ru)

Abstract. The important problem of the joint entry of hydrogen and carbon into metallic iron at high and ultrahigh pressures remains debatable. This paper presents the first results of experiments on the interaction of cementite Fe_3C with hydrogen in sealed platinum ampoules and in open sapphire ampoules at a pressure of 30-100 MPa, created by pure H_2. A comparative analysis of the experimental results showed that at hydrogen pressures (30-100 MPa) and high temperatures (1000-1150 ^oC), iron carbide actively interacts with hydrogen and almost completely decomposes to form iron and a fluid of the composition H_2+CH_4. The mass balance method in all experiments determined the concentration of volatile (H_2+CH_4) dissolved in quenching samples equal to ~ 0.70 wt. % (the average value of 4 measurements). The presence of H_2 in quenching iron samples is qualitatively confirmed on the base of the results of Raman spectroscopy, according to which weak lines of hydrogen valence oscillation are observed in the high - frequency region (4000 - 4250 cm^{-1}) of the Raman spectrum, which suggests an insignificant amount of H_2 in the sample. Gas chromatography was used to determine the composition of the fluid phase formed in experiments on the interaction of iron carbide (Fe_3C) with hydrogen at high pressures.

***Keywords**: iron carbide, hydrogen, pressures, high temperature, concentration of C and H_2, interaction*

The role of hydrogen, the most abundant element in our Galaxy, in natural processes is extremely diverse and in recent years has attracted increasing attention from petrologists and geochemists. In particular, the important problem of the co-occurrence of hydrogen and carbon in metallic iron at high and ultrahigh pressures remains debatable (Morard et al., 2017; Fei, Brosh, 2014); Narygina et al., 2011; Litasov et al., 2016; and others). This paper presents the first results of experiments on the interaction of cementite Fe3C with hydrogen in sealed platinum ampoules and in open sapphire ampoules at a pressure of 30-100 MPa, created either by pure H_2 or Ar. Special attention was paid to a thorough analysis of the composition of the fluid and metal phases formed in quenching experiments. The experiments were carried out on a unique high gas pressure apparatus. This apparatus is equipped with an original internal device, which made it possible to conduct long-term experiments at such high temperatures, despite the high penetrating power of hydrogen (Persikov et al., 2020). At the beginning of the experiment, the pressure of argon in the pressure vessel, and, accordingly, of hydrogen in the internal device, was raised within one hour to the required value - 30, 60 or 100 MPa. Next, the temperature of the experiment was raised to the required value - 1000, 1100 or 1150 ^oC. At the specified parameters, the samples were kept in automatic mode for the required time of the experiments (1 – 1.5 – 4 an hour, respectively), after which isobaric quenching was carried out with the internal heater of the installation turned off. At the same time, a sufficiently high quenching rate of the sample was achieved (~ 300 ^oC / min). The error of measuring the temperature of the experiment was ± 5 °C, and the pressure of hydrogen was ± 0.1% rel. After isobaric quenching, pressure relief in the vessel and complete cooling, the internal device was removed from the high gas pressure vessel, the ampoule with the sample was removed from the molybdenum reactor for subsequent analysis of the phases formed during the experiment. The initial sample was a large iron carbide powder (Fe_3C) synthesized in the IGM SB RAS using a unique high-pressure installation of the “BARS " type (Palyanov Yu.N., oral communication). The chemical compositions of the initial samples (Fe_3C) and the phases obtained in the experiments were determined using a digital electron X-ray microscope CamScan MV2300 (VEGA TS 5130 MM), with an attachment for energy-dispersion microanalysis INCA Energy 450 and WDS Oxford INCA Wave 700. The analyses were carried out at an accelerating voltage of 20 kV with a beam current of up to 400 nA and a spectrum set time of 50 -100 s. The carbon content in the quenched samples after the experiments (Table 1) was determined by the difference between the sums of the analyzed elements and the stoichiometric one. This C content in the samples was additionally controlled by analyzing the results of the mass balance of each experiment (Table 1). By thermal dehydration when heating sample No. 2103 after the experiment to 1000°C, the content of H_2 and CH_4 in the sample, which was preserved after isobaric quenching, was determined. The composition of the fluid phase formed in experiments in brewed platinum ampoules (Table 1) was determined by a special method of chromatography-mass spectrometric analysis on the Kristalllux-4000M device at GEOHI RAS (analyst Naimushin S. G.). Qualitative confirmation of the presence of H_2 in the quenched sample (experiment No. 2103) was performed using Raman spectroscopy (Fig. 1). Raman spectra were obtained using an RM1000 (Renishaw) spectrometer equipped with a CCD camera, an edge filter, and a Leica DMLM microscope.

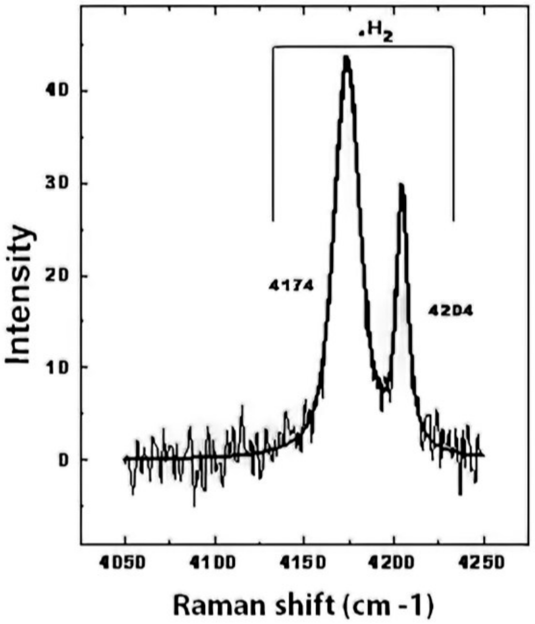

Fig. 1. Raman spectrum of sample No 2103 in the region of the valence oscillation of hydrogen.

Table 1. Parameters and results of experiments

Run No	$P(H_2)$ MPa	T, ^oC	Run time, hour	Starting material	Post-run phases	Composition of quenching fluid, vol. %	Composition of Fe_xC_y, atom. %	Note
2103	100	1000	1	Fe_3C	$Fe_xC_y + H_2 + CH_4$	$H_2 + CH_4$	X* = 98.96 У*= 1.04	Run in a brewed Pt ampoule
2109**	100	1000	1	Fe_3C	Fe_3C	Ar (100)	X*=75 У*= 25	Run in an open sapphire ampoule
2110	30	1000	1	Fe_3C	$Fe_xC_y + H_2 + CH_4$	$H_2 + CH_4$	X* = 99.02 У*= 0.98	Run in an open sapphire ampoule
2111	60	1000	1.5	Fe_3C	$Fe_xC_y + H_2 + CH_4$	$H_2 + CH_4$ $X(CH_4)$= 0.21	X* = 99.2 У*= 0.8	Run in 2 brewed Pt ampoules
2113	60	1100	1.5	Fe_3C	$Fe + H_2 + CH_4$	$H_2 + CH_4$	X* = 100 У*= 0	Run in 2 brewed Pt ampoules
2117	60	1150	4	Fe_3C	$Fe + H_2 + CH_4$	$H_2 + CH_4$	X* = 100 У*= 0	Run in 2 brewed Pt ampoules

Notes: * - Average values from 7 analyses on the microprobe. ** - Comparative run under Ar pressure.

Comparative analysis of the results of experiments 2109 and 2110 (Table.1) in open ampoules showed that at hydrogen pressures (30-100 MPa) and high temperatures (1000-1150 ^oC), iron carbide actively interacts with hydrogen and almost completely decomposes to form iron and a fluid of the composition H_2+CH_4. Whereas under Ar pressure and temperature (1000 ^oC), iron carbide remains stable without any signs of decomposition. At the experimental temperatures of 1000 °C (Table.1) C remains in small amounts in the initial phase of the sample (~1 at. %), regardless of the hydrogen pressure (30-100 MPa), and at higher temperatures, iron carbide is completely broken down and almost pure iron is formed. The mass balance method in all experiments determined the concentration of volatiles (H_2+CH_4) dissolved in quenching samples equal to ~ 0.70 wt. % (the average value of 4 measurements). The presence of H_2 in quenching iron samples is qualitatively confirmed on the basis of the results of Raman spectroscopy, according to which weak lines of hydrogen valence oscillation are observed in the high - frequency region (4000-4250 cm^{-1}) of the Raman spectrum (Fig. 1), which suggests an insignificant amount of H_2.

The presence of such lines in the high-frequency region of the RS is confirmed in a number of studies (see, for example, the work (Dalou et al., 2019). The composition of the fluid phase, formed in experiments, on the interaction of iron carbide (Fe_3C) with hydrogen at high pressures was determined, using chromatography-mass spectrometry analysis (Table 1), which was confirmed by the corresponding thermodynamic analysis (Fig. 2). The reaction controlling the interaction of Fe3C with hydrogen:

$$Fe_3C + 2H_2 = Fe_xC_{(1-x)} + CH_4 \qquad (1)$$

and the equilibrium constant of this reaction (1):

$$K\ (1) = f(CH_4)*a(C, metal)/f2(H_2) \qquad (2).$$

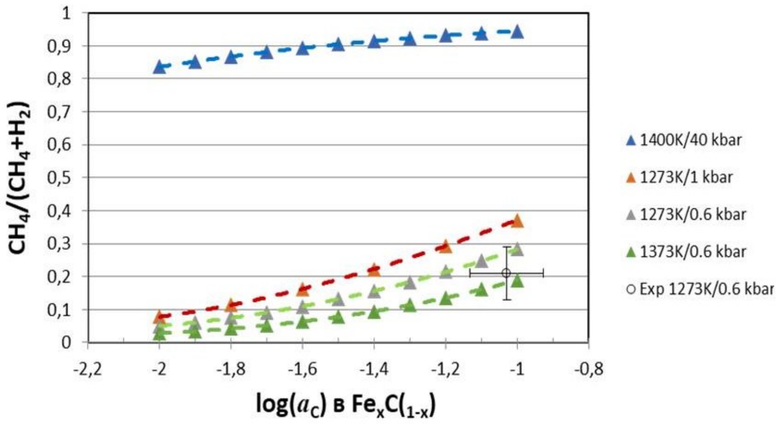

Fig. 2. The molar fraction of methane in the CH_4-H_2 fluid in equilibrium with the Fe—C metal phase with variable content (and activity) of C.

The properties of the fluid are calculated from the work (Aranovich, 2013). The activity of C in the experimental sample is calculated by the equation from the work (Fei, Brosh, 2014) for the composition $Fe_{0.986}C_{0.014}$, measured on a microprobe. The composition of the fluid X (CH_4) = 0.21, according to chromatography-mass spectrometry analysis.

References

Aranovich L. Y. (2013). Fluid–Mineral Equilibria and Thermodynamic Mixing Properties of Fluid Systems. Petrology, 21, 539–549.

Dalou C., Hirschmann, M.M. Jacobsen, S.D. Le Losq C. (2019). Raman spectroscopy study of C-O-H-N speciation in reduced basaltic glasses: Implications for reduced planetary mantles. Geochimica et Cosmochimica Acta, V. 265, 32-47.

Fei Y., Brosh E. (2014). Experimental study and thermodynamic calculations of phase relations in the Fe–C system at high pressure. Earth and Planetary Science Letters, 408, 155–162.

Litasov K.D., Shatskiy A.F., Ohtani E. (2016). Interaction of Fe and Fe_3C with Hydrogen and Nitrogen at 6–20 GPa: a Study by in Situ X-Ray Diffraction. Geochem. Inter., 54, 914–921

Morard G., Andrault D., Antonangeli D., et al. (2017). Fe–FeO and Fe–Fe_3C melting relations at Earth's core–mantle boundary conditions: Implications for a volatile-rich or oxygen-rich core. Earth and Planetary Science Letters, 473, 94–103.

Narygina, O., Dubrovinsky, L. S., McCammon, C. A., et al. (2011). X-ray diffraction and Meossbauer spectroscopy study of fcc iron hydride FeH at high pressures and implications for the composition of the Earth's core. Earth and Planetary Science Letters, 307, 409–414.

Persikov E. S., Bukhtiyarov P. G., Aranovich L. Ya., Shchekleina M.D. (2020). Features of hydrogen interaction with basaltic melts at pressures 10 - 100 MPa and temperatures 1100 – 1250 °C. Chemical Geol., v. 556, p. 5 December. DOI: ttps://doi.org/10.1016/j.chemgeo.2020.119829.

Persikov E.S., Bukhtiyarov P.G. Viscosity of heterogeneous basalt melts under hydrogen pressure.

IEM RAS. Chernogolovka. (persikov@iem.ac.ru)

Abstract. The viscosity of heterogeneous basalt melts was estimated using a new structural – chemical model for reliable calculations of the temperature, concentration, phase, and pressure dependences of magma viscosity (Persikov, Bukhtiyarov, 2020). It was made in the temperature range of 1100-1300 °C, hydrogen pressures of 10-100 MPa, and metal phase concentrations up to 10 vol. %, crystal concentrations up to 30 vol. % and bubble concentrations up to 40 vol.%. It is found that the concentration of crystals, the metal phase, and bubbles in the melt has the greatest influence on the viscosity of such melts. For example, when their total concentration in the melt is equal to 80 vol. %, the viscosity of the basalt melt increases by almost an order of magnitude in the full range of the specified temperatures.

Keywords: *viscosity, basalt, hydrogen, pressures, temperature, crystals, babbles, metal phase*

In continuation of experimental and theoretical studies of the interaction of basalt magmas with hydrogen (Persikov et al., 2019; 2020), the viscosity of basalt melts formed during this interaction was studied. It was found that as a result of the hydrogen-magmatic interaction, initially homogeneous basalt melts become heterogeneous (Persikov et al., 2019; 2020). They form inclusions of the metallic phase (Fe, FeNiCo alloys), H_2O, crystals of high-magnesian olivines and pyroxenes, and bubbles of the fluid phase. The viscosity of such melts was estimated using a new structural-chemical model for reliable calculations of the temperature, concentration, phase, and pressure dependences of magma viscosity (Persikov and Bukhtiyarov, 2020). The calculation was made in the temperature range of 1100 – 1300 °C, hydrogen pressures of 10 -100 MPa, metal phase concentrations up to 10 vol. %, and crystal concentrations up to 30 vol. % and bubble concentrations up to 40 vol.%. The composition of the initial melt of magnesian basalt and its composition after the experiment under hydrogen pressure, along with the structural and chemical index of the basicity of the melts (100NBO/T) is presented in Table 1. The results of calculations of the viscosity of heterogeneous basalt melts when they interact with hydrogen at a pressure of 100 MPa are presented in Table 2 and in Figure 1. It is established that the temperature dependence of such melts is fairly correctly described by the well - known theoretical Arrhenius—Frenkel—Eyring equation (for example, Persikov, Bukhtiyarov, 2004):

$$\eta = \eta_o \exp (E/RT) \qquad (1)$$

with a constant value of the pre-exponential factor $\eta_o = (10^{-4.5} \pm 10^{-0.1})$ Pa s. It made it possible for the first time to obtain reliable values of the activation energy of a viscous flow of such melts (E = 160 kJ/mol), which has a clear physical meaning, as a potential barrier or a change in the free energy of the system during the flow. It is also found that the concentration of crystals, the metal phase, and bubbles in the melt has the greatest influence on the viscosity of such melts. So, for example, when their total concentration in the melt is equal to 80 vol. % the viscosity of the basalt melt increases by almost an order of magnitude over the full temperature range (Table 2).

Table 1. Chemical compositions (wt. %) and structural-chemical parameters (100NBO/T) of the initial magnesian basalt and magnesian basalt after its interaction with hydrogen

Components	After runs 2098-2100*	Starting basalt**
SiO_2	53.49	49.5
Al_2O_3	14.21	13.18
Fe_2O_3	0.00	3.18
FeO	5.74	6.85
MnO	0.24	0.15
MgO	9.62	9.98
CaO	12.12	12.34
Na_2O	2.56	2.18
K_2O	0.92	0.93
TiO_2	1.11	1.01
P_2O_5	not found	0.25
H_2O+	not found	not found
OH^-	0.95	0.29
NiO	0.09	not found
Co_3O_4	0.11	not found
Sum	101.2	99.84
100NBO/T	84	83

Note: * - the average composition in experiments with melts of the initial magnesian basalt with NiO and Co_3O_4, P (H_2) = 100 MPa, T =1100 -1300 °C. ** - magnesian basalt, northern breakthrough (the Great Tolbachin fissure eruption of 1975-1976, Kamchatka, 1984).

Table 2. Results of calculations of the viscosity of heterogeneous basalt melts interacting with hydrogen.

P(H_2), MPa	T, ^oC	Log η_T^P, η_T^P - Pa s	Vcr.+ Vmet., vol. %	Vb., vol. %
100	1100	2,6	30 + 10	40
100	1200	2,1		
100	1300	1,8		
100	1100	2,0	10 +10	20
100	1200	1,6		
100	1300	1,2		
100	1100	1,6	0	0
100	1200	1,2		
100	1300	0,8		

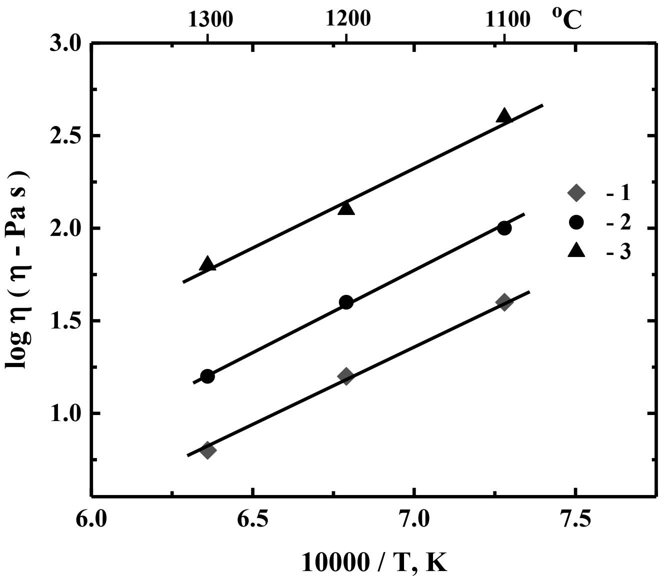

Fig. 1. Isobaric temperature dependence of the viscosity of heterogeneous basalt melts when interacting with hydrogen at a pressure of 100 MPa.

1 - homogeneous melt without crystals, metal separations and bubbles in the melt; 2 – the total concentration of crystals, metal separations and bubbles in the melt is 40 vol.%; 3 - the total concentration of crystals, metal separations and bubbles in the melt is 80 vol. %.

References

Bolshoe fissure Tolbachinskoe eruption 1975-1976, Kamchatka (1984) Moscow: Nauka, 637 p. (in Russia).

Persikov E. S., Bukhtiyarov P.G. (2004) Experimental study of the influence of lithostatic and water pressure on the viscosity of silicate and magmatic melts. A new structural-chemical model for calculating and predicting their viscosity // Experimental mineralogy, some results at the turn of the century. Edited by V. A. Zharikov, V. V. Fedkina. M., Nauka, vol. 1, p. 103-122 (in Russia).

Persikov E. S, Bukhtiyarov P.G., Aranovich L.Y., Nekrasov A.N., Shaposhnikova O.Yu. (2019). Experimental modeling of the formation of native metals in the earth's crust in the interaction of hydrogen with basalt melts. Geochemistry International. v. 57, No 10, p. 1035-1044. DOI: 10.1134/S0016702919100082

Persikov E. S, Bukhtiyarov P. G. (2020). Viscosity of magmatic melts: Improved structural - chemical model. Chemical Geol., v. 556, p., 5 December. DOI: https://doi.org/10.1016/j.chemgeo.2020.119820,.

Bukhtiyarov P.G., Persikov E.S. Study of the comparative effect of high pressures H_2 and Ar (up to 400 MPa) on the viscosity of albite and andesite melts at temperatures of 1200-1400 °C

IEM RAS. Chernogolovka. (pavel@iem.ac.ru)

Abstract. Experimental data on the effect of high hydrogen pressures on the viscosity of magmatic melts are practically absent. This paper presents the results of studying the temperature and pressure dependences of the viscosity of albite and andesite melts at hydrogen and argon pressures of 400 MPa in the temperature range of 1200 -1400 °C. It is established that the temperature dependence of the viscosity of albite and andesite melts under the pressure of hydrogen and argon is quite correctly described by the well—known theoretical Arrhenius-Frenkel-Eyring equation. For the first time, reliable values of the activation energies of the viscous flow of albite and andesite melts at high pressures of hydrogen were obtained. It is shown that the viscosity of the studied melts decreases linearly under isothermal conditions with an increase the pressure of argon and hydrogen.

Keywords: *viscosity, albite, andesite melts, hydrogen, argon, pressures, temperature*

Experimental data on the effect of high hydrogen pressures on the viscosity of magmatic melts are practically absent. This paper presents the results of studying the temperature and pressure dependences of the viscosity of albite and andesite melts at hydrogen and argon pressures of 400 MPa in the temperature range of 1200-1400 °C. Taking into account previously obtained data on the viscosity of albite and andesite melts at atmospheric pressure (Bukhtiyarov et al., 1987; Persikov et al., 1990; Persikov, 1998). The experiments were carried out using a high gas pressure apparatus containing a unique internal device that allows experiments on the viscosity of melts at high temperatures and pressures of argon or hydrogen without changing the geometry of the ampoule with the melt during the experiments. Natural albite (Kalba deposit, Kazakhstan) and andesite from the Avacha volcano in Kamchatka were used as starting samples for viscosity measurements. The glasses required for the subsequent measurement of the melt viscosity were synthesized by melting albite and andesite powders in open platinum ampoules at T = 1400 °C and atmospheric pressure. The chemical compositions of the albite and andesite melts (glasses) are shown in Table 1, along with their degree of depolymerization (100NBO/T). The compositions of these glasses and their homogeneity were determined using a digital electron X-ray microscope Vega TS 5130MM (CamScan MV2300) with an attachment for energy-dispersion microanalysis INCA Energy 200. The viscosity of albite and andesite melts at high pressures of argon and hydrogen was measured by the quenching method of a falling sphere using platinum-rhodium spheres (Pt60Rh40) with a diameter of (200-300) microns. The rate of their fall in the melts was determined by the time each sphere traveled a certain distance in the melt at the required temperature and pressure values in the experiment. The time was measured from the moment of reaching the desired T, P - parameters to the moment of isobaric quenching of the melt, and the distance traveled by the sphere in the melt during this time was determined in the quenched samples under a microscope.

Table 1. Compositions of melts (glasses, wt. %) and their structural-chemical parameter (100NBO/T)

Components	Andesite	Andesite + H_2	Ab	Ab + H_2
SiO_2	58.56	58.43	68.73	68.7
TiO_2	0.64	0.63	-	-
Al_2O_3	18.08	18.08	19.45	19.44
Fe_2O_3	1.06	1.06	-	-
FeO	6.8	6.8	-	-
MnO	0.15	0.13	-	-
MgO	3.48	3.48	-	-
CaO	6.32	6.32	-	-
Na_2O	3.54	3.54	11.82	11.81
K_2O	0.92	0/92	-	-
P_2O_5	-	-	-	-
OH^-	-	0.8	-	0.05
∑	99.4	100.2	100	100
100NBO/T	26.1	33.4	0.02	0.4

The viscosity of melts at specified T, P - parameters of the experiment was calculated according to the well-known Stokes' law with the amendment Faxen on the parietal effect (Persikov, 1998):

$$\eta = 2g\, r^2\Delta\rho/9V(1+3.3r/h) \times [1-2.104r/r_a+2.09(r/r_a)^3 - 0.95(r/r_a)^5] \qquad (1)$$

where: r is the radius of the sphere; r_a – the inner radius of the platinum vial melt; h – the height of the capsule; g – acceleration of gravity; Δρ - the difference between the densities of the sphere and melt; V – velocity of the falling sphere in the melt; η - the viscosity of the melt at T, P – parameters of the run, Pa s.

The density of the melts was assumed to be equal to the densities of the melts quenched under isobaric conditions, the densities of which were obtained by hydrostatic weighing after experiments. The calculated total error in measuring the viscosity of the melts did not exceed ± 30 rel. %.

It was experimentally established that the temperature dependence of the viscosity of albite and andesite melts under pressure of hydrogen and argon (Fig. 1) is quite correctly described by the well-known theoretical Arrhenius-Frenkel-Eyring equation (for example, Persikov, Bukhtiyarov, 2004):

$$\eta = \eta_o \exp (E/RT) \qquad (2)$$

with a constant value of the pre-exponential factor $\eta_o = (10^{-4.5} \pm 10^{-0.1})$ Pa s, which made it possible for the first time to obtain reliable and comparable values of the activation energy of the viscous flow (E, equation 2) of such melts (Table 2). It has a clear physical meaning, as a potential barrier or a change in the free energy of the system during the viscous flow.

The dependence of the viscosity of albite and andesite melts on the pressure of hydrogen and argon is shown in Fig. 2. From the analysis of these results, it follows that the viscosity of the studied melts decreases linearly under isothermal conditions with an increase in the pressure of argon and hydrogen (T = 1300 ^{o}C). At the same time, it was found that within the experimental error (± 30 rel. %) the viscosity of albite melts (without elements of variable valence) under a hydrogen pressure of 400 MPa is comparable to their viscosity under argon pressure in the full temperature range of experiments.

Whereas the viscosity of andesite melts with elements of variable valence (Fe) under a hydrogen pressure of 400 MPa decreases to a much greater extent than their viscosity under argon pressure (Fig. 1, 2). This is due to water (Table 1), which is formed in andesite melts when they interact with hydrogen due to the reduction of oxides of variable valence.

For the first time, reliable values of the activation energies of the viscous flow of albite and andesite melts at high pressures of hydrogen and argon were obtained (Table 2).

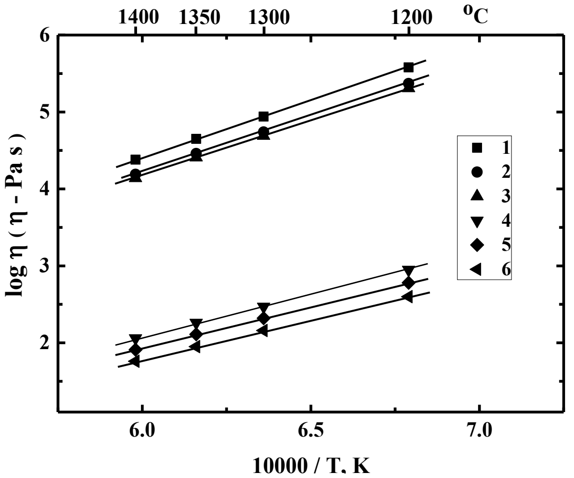

Fig. 1. Temperature dependence of the viscosity of albite and andesite melts. 1 – albite melt, P = 1 atm; 2 - albite melt, P (Ar) = 400 MPa; 3-albite melt, P (H_2) = 400 MPa; 4 - andesite melt, P = 1 atm; 5 - andesite melt, P (Ar) = 400 MPa; 6 - andesite melt, P (H_2) = 400 MPa.

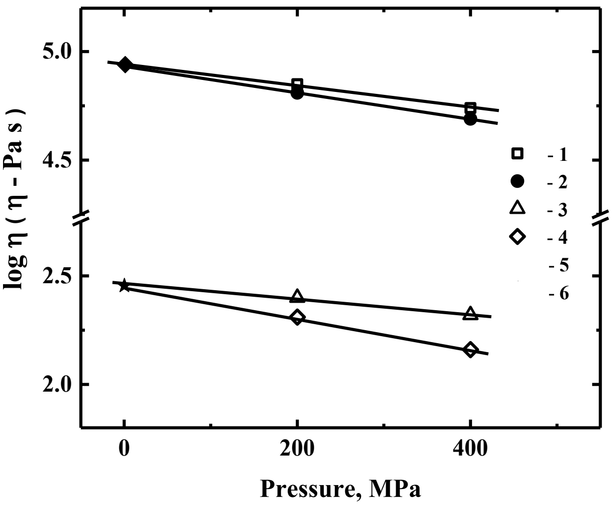

Fig. 2. Isothermal (1300 °C) dependence of the viscosity of the melts of albite and andesite on the pressure.
1- albite melt, P (Ar); 2 - albite melt, P(H_2); 3 - andesite melt, P(Ar); 4 - andesite melt, P(H_2); 5 - albite melt, P = 1 atm; 6 - andesite melt, P = 1 atm.

Table 2. Parameters and results of experiments

Melt	**P [MPa]**	**T [°C]**	**Log η [η, Pa s]**	**E [kJ/mol]**
Albite	0.1	1200	5.58 ± 0.14	283.8 ± 2.8
Albite	0.1	1300	4.94 ± 0.13	283.8 ± 2.8
Albite	0.1	1350	4.65 ± 0.12	283.8 ± 2.8
Albite	0.1	1400	4.38 ± 0.11	283.8 ± 2.8
Albite + Ar	400	1200	5.37 ± 0.15	277.8 ± 2.7
Albite + Ar	400	1300	4.74 ± 0.14	277.8 ± 2.7
Albite + Ar	400	1350	4.46 ± 0.11	277.8 ± 2.7
Albite + Ar	400	1400	4.19 ± 0.13	277.8 ± 2.7
Albite + H_2	400	1200	5.31± 0.15	276.2 ± 2.7
Albite + H_2	400	1300	4.69 ± 0.13	276.2 ± 2.7
Albite + H_2	400	1350	4.41 ± 0.12	276.2 ± 2.7
Albite + H_2	400	1400	4.14 ± 0.11	276.2 ± 2.7
Andesite	0.1	1200	2.95 ± 0.14	210 ± 2.1
Andesite	0.1	1300	2.47 ± 0.13	210 ± 2.1
Andesite	0.1	1350	2.26 ± 0.13	210 ± 2.1
Andesite	0.1	1400	2.06 ± 0.12	210 ± 2.1
Andesite + Ar	400	1200	2.78± 0.15	205 ± 2.0
Andesite + Ar	400	1300	2.32 ± 0.14	205 ± 2.0
Andesite + Ar	400	1350	2.11 ± 0.13	205 ± 2.0
Andesite + Ar	400	1400	1.91 ± 0.12	205 ± 2.0
Andesite + H_2	400	1200	2.6 ± 0.14	200 ± 2.0
Andesite + H_2	400	1300	2.16 ± 0.13	200 ± 2.0
Andesite + H_2	400	1350	1.95 ± 0.13	200 ± 2.0
Andesite + H_2	400	1400	1.76± 0.12	200 ± 2.0

References

Bukhtiyarov P. G., Persikov E. S., Kalinicheva T. N. (1987) Viscosity of andesite melts. Volcanology and Seismology, No. 5, p. 45-53 (in Russia)

Persikov E. S., Zharikov V. A., Bukhtiyarov P. G., Pol'skoy S. F. (1990) The effect of volatiles on the properties of magmatic melts. Eur. J. Mineral. (2):621-642.

Persikov E.S. (1998) Viscosity of model and magmatic melts at the pressures and temperatures of the Earth's crust and upper mantle. Russian Geology and Geophysics 39(11), 1780-1792.

Persikov E. S., Bukhtiyarov P. G. (2004) Experimental study of the influence of lithostatic and water pressure on the viscosity of silicate and magmatic melts. A new structural-chemical model for calculating and predicting their viscosity. In: Experimental mineralogy, some results at the turn of the century. Edited by V. A. Zharikov, V. V. Fedkina. M., Nauka, vol. 1, p. 103-122 (in Russia).

Khodorevskaya L.I., Varlamov D.A. Interaction of amphibol with H_2O-NaCl-KCl fluid at 750°C, 700 MPa: features of the composition of mineral phases and melts UDC 553.065.1

D.S. Korzhinskii Institute of Experimental Mineralogy RAS, Chernogolovka Moscow district. (khodorevskaya@mail.ru; dima @iem.ac.ru). Tel.: +79166512553.

Abstract. The interaction of amphibole with (K,Na)Cl-H_2O solutions was studied experimentally at T=750°C, P=700 MPa with high and varying salt concentrations. At low $X_{KCl}/(X_{KCl}+X_{NaCl})$ ratios in fluid, *Hbl+Ne+Sdl+Pl+Bt±Cpx* associations are stable. An increase in the ratio results in unstable *Ne, Sdl, Pl* and *Hbl*. At an $X_{KCl}/(X_{KCl}+X_{NaCl})$ ratio over 0.5, the association *Cpx+Bt+Kfs+Grt* (grossular-andradite) is stable. Thus, high sodium activity is indicated by nepheline and high potassium activity - by garnet of *Grs-Andr* composition. The appearance of *Grs-Andr* supports conclusions of the genesis of sviatonossites in which high a_K fluids were involved. As the bulk salinity of fluids decreases and a_{H2O} (a_{H2O}>0.4) increases, melts are formed whose composition varies from trachytes to phonolites. As X_{KCl} grows as part of a fluid phase, the alumina content of the melts decreases. As the total salinity of the fluid rises, the potassium content of the melt increases and its chlorine content decreases.

***Keywords**: amphibole, NaCl, KCl, alkali metasomatism, fluid, grossular, andradite, nepheline*

Numerous studies conducted in the past few decades indicate that salt chlorides, together with H_2O and CO_2, are involved in high temperature metamorphism and metasomatism. K, Na and Ca chlorides are especially important (Newton, Manning, 2010 and references therein). Estimates of chloride concentrations in high-temperature fluids are highly variable. High Na and K chloride concentrations in fluids markedly decrease H_2O activity (Aranovich, Newton, 1996), but transporting properties persist and even become stronger than those of the fluids of H_2O–nonpolar gas systems. In addition to total salinity, a K/Na ratio in fluid is highly essential. Under $(Na_2O+K_2O)<Al_2O_3$ conditions (metaaluminium type of rocks), variations in K/Na in fluid are responsible for either rock granitization with corresponding mineral associations or charnockitization. Under $(Na_2O+K_2O)>Al_2O_3$ conditions (peraluminium type), variations in a K/Na ratio in magmatic fluid trigger the formation of alkaline magmatic rocks from leucitic to nepheline phonolites. Studies (Aranovich et al., 2013) have shown that a K/Na ratio in fluid is an essential factor which provokes melting. The interaction of fluids, which contain elevated K and Na salt concentrations, with rocks is also indicated by metasomatism. Variations in alkali activity in fluids are responsible for the geochemical pattern of the transport and redeposition of REE and trace elements.

The goal of this contribution was to identify and study the compositions of the phases forming in an amphibole-NaCl-KCl-H_2O system. The data obtained will re-assess and update available evidence for metasomatism provoked by fluids with high alkali activities.

Experiments were conducted following an ampoule procedure on standard high gas pressure equipment at a temperature of 750°C and a pressure of 700 MPa. Natural amphibole (tschermakite) was used as reference material. A fluid phase was preset by a variable NaCl/ KCl/H_2O ratio. Ampoules were sealed and kept in an experimental regime for 7-14 days. The detailed procedure, as well as the course of the experiments and phase analysis after the experiments are described in (Khodorevskaya, Aranovich, 2016).

Complete chemical equilibrium in minerals after the experiments was not always reached, as evidenced by the formation of zonal amphibole and biotite grains provoked by the preferential redistribution of Fe from mineral to fluid. Similarly, plagioclase was incompletely replaced by K-feldspar (*Pl→Kfs*). Attempts to obtain homogeneous non-zonal minerals by increasing the duration of the experiments from seven to fourteen days have failed. Fine amphibole grains, less than 50 μm in size, were mostly non-zonal and consistent in composition with the marginal zones of coarse grains. Studies (Helz, 1973 et al.) have also shown that the system is not fully equilibrated at temperatures of 700–900°C and pressures of 300–700 MPa in metabasic rock – H_2O systems when the length of experiments is increased to seven days.

In a (Na,K)Cl-H_2O system, the formation of mineral associations at preset *PT*- parameters is controlled by water activity, a_{H2O}, (X_{H2O}) and an $X_{KCl}/(X_{KCl}+X_{NaCl})$ ratio in fluid.

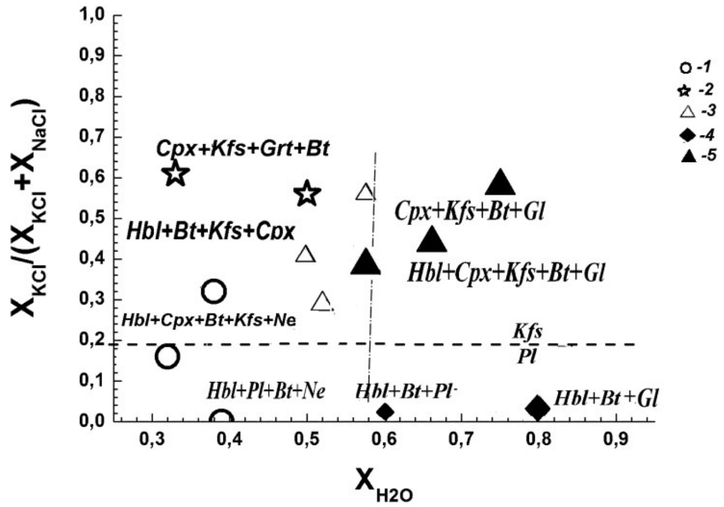

Fig.1. Mineral associations after experiments at X_{H2O} – ($X_{KCl}/(X_{KCl}+X_{NaCl})$ ratios preset in the experiments: 1 – *Ne+Hbl+Bt+Pl±Kfs±Cpx*; 2 – *Grt±Hbl+Bt+Kfs+Cpx*; 3 – *Hbl+Bt+Cpx+Kfs*; 4 – *Glass* + *Hbl+Bt+Pl*; 5 – *Glass+Hbl+Cpx+Bt+Kfs*.

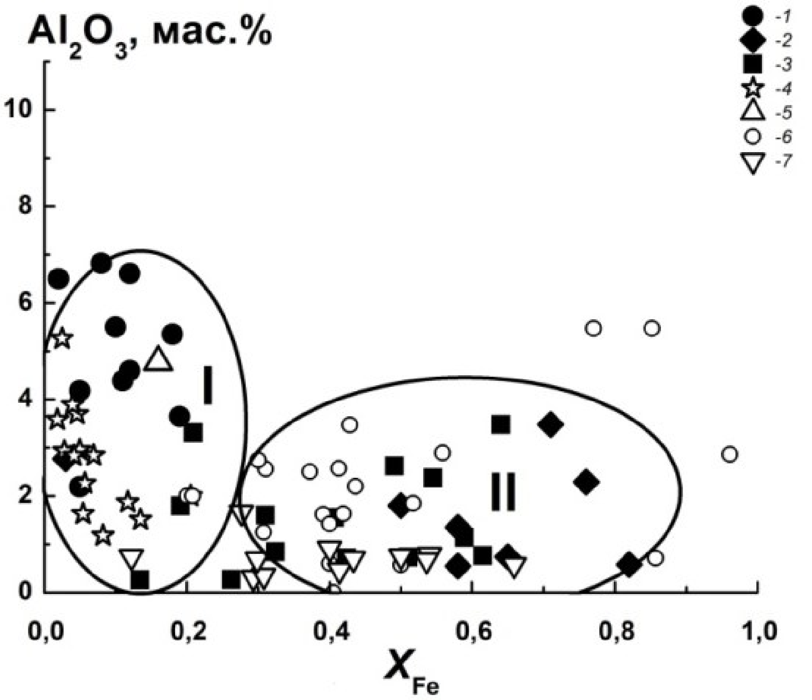

Fig. 2. X_{Fe} – Al_2O_3 concentration (mas. %) ratio in pyroxenes from the experimental and natural samples. 1-3 experimental data: 1 – in Cpx of the present study, 2 – data (Khodorevskaya, 2020), 3 – (Safonov et al., 2014), 4-7 – in natural objects: 4 – (Starikova, 2013), 5 – (Nemov, 2020), 6 – (Levin, 1974), 7 – (Kozlov, Arzamastsev, 2015).

Shown in Fig. 1 are major mineral associations formed experimentally. Such minerals as *Hbl, Cpx, Bt* and *Kfs* are characteristic of most experiments, while nepheline/sodalite, garnet and hardening melt (*Glass*) are stable at certain salt component ratios. According to (Aranovich et al., 2013), the stability field *Pl* is limited by a $X_{KCl}/(X_{KCl}+X_{NaCl})<0.2$ ratio in a fluid phase (a horizontal dashed line in the Fig. 1). At higher Na and K chloride ratios in fluid, plagioclase may persist only as inclusions in *Kfs*. Similarly, *Hbl* is unstable at high X_{KCl}. High a_{H2O} I fluid ($X_{H2O} \geq 0.6$) will be responsible for the partial melting of amphibole. The presence of melt in experimental products is indicated by a vertical line and shaded symbols in Fig. 1.

Clinopyroxenes form in practically all experiments. Compositionally, they are part of a Ca-Fe-Mg (*Quad*) group. The average iron content of the mineral ($X_{Fe} = X_{Fe}/(X_{Fe}+X_{Mg}) \leq 0.3$), is 0.10-0.15. A distinctive feature of *Cpx* is highly variable (1-3 to 7 mas. %) Al_2O_3 concentration, which is observed occasionally in the same experiment. Al_2O_3 concentration in *Cpx* seems to be due to isomorphism of tschermakite's type isomorphism based on the scheme $Mg^{2+}(Fe^{2+}) + Si^{4+} = 2Al^{3+}$ in highly saline solutions, as has been noted earlier in (Khodorevskaya, Aranovich, 2016).

Shown in Fig. 2 is a X_{Fe} – Al_2O_3 ratio in *Cpx* obtained experimentally (dark symbols) and in *Cpx* from natural alkaline metasomatic rocks (light symbols). Field I displays low X_{Fe}^{Cpx} values and high Al_2O_3 concentrations. The field contains the data obtained in the present study. Higher X_{Fe}^{Cpx} values and low Al_2O_3 concentrations (field II) were obtained in (Safonov et al., 2014), where the composition of the reference solution was preset by H_2O, CO_2 ($X_{CO2} = 0.494$) and low salinity, $X_{NaCl}+X_{KCl}< 0.1$. In studies (Khodorevskaya, 2020) the fluid consisted of H_2O-Na_2CO_3 (Fig. 2). The alkaline-carbonate fluid reproduced in (Safonov et al., 2014; Khodorevskaya, 2020) seems to be responsible for the formation of iron-richer *Cpx* with lower Al_2O_3 concentration.

Fig. 2 shows that a X_{Fe} – Al_2O_3 ratio in natural *Cpx* from alkaline metasomatic rocks and nepheline syenites could be regarded as part of both field I and field II (Starikova, 2013; Nemov, 2020; Levin, 1974; Kozlov, Arzamastsev, 2015 et al.). The above experimental data suggest that clinopyroxenes of *Quad* composition indicate that they formed in the presence of metasomatizing fluid in which they dominated KCl, NaCl. The presence of alkaline-carbonate-fluid gave rise to clinopyroxenes with higher *f*.

All of the amphiboles formed in the experiments are in a group of calcium amphiboles (Fig. 3). An increase in X_{NaCl} in the reference fluid results in the replacement Ca → Na, but Ca-Na amphiboles амфиболы did not appear at any initial X_{NaCl} values. As a result of isomorphic replacements, $({}^{(A)}+{}^{(6)}Mg + 2{}^{(4)}Si) = ({}^{(A)}Na + 2{}^{(4)}Al + {}^{(6)}Al)$ and $({}^{(A)}+{}^{(6)}Mg + 2{}^{(4)}Si) = ({}^{(A)}Na + 2{}^{(4)}Al + {}^{(6)}Fe^{3+})$, initial tschermakite in the experiments turned into pargasite – hastingsite. The iron content of the mineral decreases from $X_{Fe} \approx 0.30$-0.40 in the centers to $X_{Fe} \approx 0.20$-0.30 towards grain margins. An iron rim, $X_{Fe} \approx 0.90$, forms along the margins of some amphiboles.

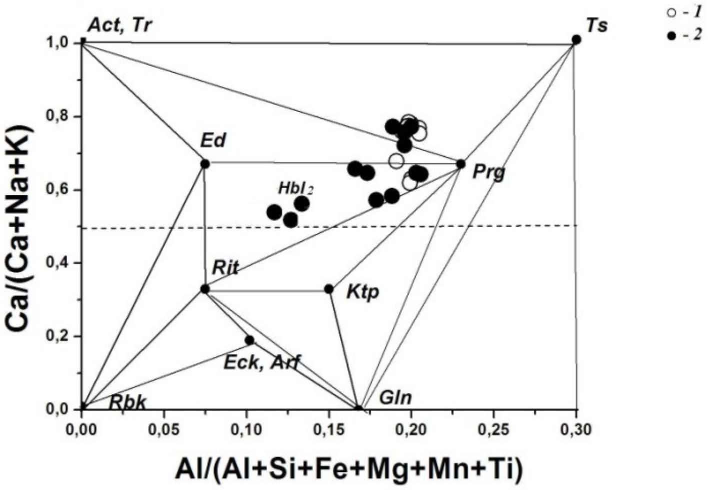

Fig. 3. Al/(Al+Si+Fe+Mg+Mn+Ti) – Ca/(Ca+Na+K)K/(K+Na) ratio in amphiboles; The dashed line separates Ca-amphiboles from Ca-Na amphiboles: 1 – 2 – values for the centres and margins of minerals, respectively.

Amphibole margins exhibit a direct correlation between X_{KCl} in fluid and potassium concentration in amphiboles expressed by the ratio: $X_K^{Hbl} = 0.13 + 0.90\ X_{KCl}(fluid) + 0.12X_{KCl}^2\ (fluid)$. No relation of X_{NaCl} (fluid) – X_{Na} (*Hbl*) type is displayed. Titanium concentration in amphiboles from grain centers to grain margins after the experiments remains practically unchanged. Chlorine is not part of the mineral.

At low H_2O activity ($a_{H2O} < 0.35$-0.40) and a $X_{KCl}/(X_{KCl}+X_{NaCl})$ ratio in the fluid determined as $X_{NaCl}=0.506$-$0.84X_{KCl}$ the formation of nepheline takes place (Fig. 1). The potassium content of nepheline is correlated with a mole X_{KCl} fraction in the fluid, and can be expressed by the equation:: $X_K(Ne) =0.007+0.837\ X_K\ (fluid) - 0,692\ [X_K\ (fluid)]^2$.

At a $X_{KCl}/(X_{KCl}+X_{NaCl})$ ratio ≥ 0.5 (Fig.1), garnet of andradite-grossular series is stable. Experimentally obtained *Grs-Andr* associations with the minerals *Kfs, Pl, Cpx* (*Di-Hd*), high-Fe *Hbl* and sometimes with *Ne* are similar to the mineral parageneses of sviatonossites – interesting rocks of limited global distribution but widespread in the Baikal region (Levitsky et al., 2012). According to the authors, svyatonosites display the highest alkaline metal concentration, in which K_2O dominates over Na_2O. They formed in high-calcium settings such as marbles and gabbroic rocks. High potassium activity in the fluid upon the formation of these rocks was also observed in (Makrygina, 2008 et al.).

Thus, high potassium activity in all fluids is indicated by garnet of *Grs-Andr* composition and high sodium activity by nepheline. Such minerals as clinopyroxenes and amphiboles primarily indicate the cation-anion composition of fluid, although a certain degree of metamorphism Na → K in amphiboles and Ca → Na in clinopyroxenes is observed.

At $a_{H2O} > 0.40$, the partial melting of ampbibole takes place together with newly-formed *Cpx, Bt* and *Kfs*. The composition of the melts is consistent with that of phonolites. As the total salinity of the fluid in the melt increases, its chlorine content decreases, i.e sodium melts are richer in chlorine than potassic.

The experiments have shown that upon the interaction of amphibole with fluids containing high NaCl and KCl salt concentrations, mineral associations characteristic of the alkaline metasomatism of amphibole rocks are formed.

This study was carried out under government financed project AAAA-A18-118020590148-3 for the Korzhinskii Institute of Experimental Mineralogy, Russian Academy of Sciences.

References

Aranovich L.Y., Newton R.C. H_2O activity in concentrated NaCl solutions at high temperatures and pressures measured by the brucite–periclase equilibrium // Contrib. Mineral. Petrol. – 1996. V. 125. No.2-3. – P.200-212. DOI: 10.1007/s004100050216

Aranovich, L. Y., Newton, R. C., Manning, C. E. Brine-assisted anatexis: Experimental melting in the system haplogranite- H_2O-NaC-KCl at deep-crustal conditions // Earth and Planetary Science Letters. – 2013. V. 374. – P.111-120. DOI: 10.1016/j.epsl.2013.05.027

Helz R.T. Phase relations of basalts in their melting ranges at P = 5 kb as a function of oxygen fugacity. Part I. Mafic phases // J. Petrol. – 1973. V. 14(2). – P. 249-302. DOI: 10.1093/petrology/14.2.249

Khodorevskaya L.I. Experimental modelling of alkaline metasomatism under pressure gradient conditions at 750°C // Experiment in Geosciences. – 2020. V. 26, № 1. – P. 149-152.

Khodorevskaya L.I., Aranovich L.Y. Experimental study of amphibole interaction with H_2O-NaCl Fluid at 900°C, 500 MPa: toward granulite facies melting and mass transfer // Petrology. –2016. V. 24, No. 3. – P. 215-233. DOI: 10.1134/S0869591116030036

Kozlov E.N., Arzamastsev A.A. Petrogenesis of metasomatic rocks in the fenitized zones of the Ozernaya Varaka alkaline ultrabasic complex, Kola Peninsula// Petrology. 2015. – V.23. № 1. – P.45-67. DOI: 10.1134/S0869591115010026

Leake B.E., Woolley A.R., Birch W.D. et al. Nomenclature of amphiboles. Report of the Subcommittee on Amphiboles of the International Mineralogical Association Commission on New Minerals and Mineral Names // Eur. J. Mineral. – 1997. V. 9(3). – P. 623-651. DOI: 10.1127/ejm/9/3/0623

Levin V.Ya. The alkaline province of the Ilmen Vishnevye Mountains (Uralian nepheline syenite formation). – M., Nauka. 1974. (*in Russian*)

Levitsky V. I., Reznitsky L. Z., Sklyarov E. V., Levitsky I. V., Kovach V. P., Makagon V. M. Svyatonosites of Eastern Siberia - products of the cow-mantle interaction // Materials of reports of the All-Russian Meeting "Modern problems of geochemistry".– Irkutsk: IG SB RAS, 2012. – V. 2. –P. 150-152. (*in Russian*)

Makrygina V.A., Petrova Z.I., Koneva A.A., Suvorova L.F. Composition, P-T parameters, and metasomatic transformations of mafic schists of the Svyatoi Nos peninsula, Eastern Baikal area // Geochemistry International. –2008. –V. 46. № 2. – P.140-155. DOI: 10.1007/s11476-008-2004-8

Nemov A. B. Garnet-Amphibole Miaskites of the Ilmenogorsky Miaskite Massif (Southern Urals): Mineralogy and Geochemistry // Litosphere. –2020. – V 20, № 5. –P. 652–667 (*In Russian*). DOI: 10.24930/1681-9004-2020-20-5-652-667

Newton R.C., Manning C.E. Role of saline fluids in deep crustal and upper_mantle metasomatism: insights from experimental studies // Geofluids. – 2010. V.10. – P.58-72. DOI: 10.1111/j.1468-8123.2009.00275.x

Safonov O.G., Kosova S.A., van Reenen D.D. Interaction of Biotite–Amphibole Gneiss with H_2O–CO_2–(K, Na)Cl Fluids at 550 MPa and 750 and 800°C: Experimental Study and Applications to Dehydration and Partial Melting in the Middle Crust // J. Petrol. – 2014. V. 55(12). – P. 2419–2456. DOI: 10.1093/petrology/egu062

Starikova A. E. Mineralogy of metasomatic rocks of the Tazheran massif (Western Baikal Region) // Ph.D. thesis abstract, – Novosibirsk, 2013. – 21 p. (*In Russian*)

Novoselov I.D.[1,2], Palyanov Yu.N.[1,2], Borzdov Yu.M.[1] Experimental modeling of lherzolitic and eclogitic garnets carbonation in CO_2 and CO_2-H_2O fluids at 6.3 GPa and 950-1250 °C

[1] Sobolev Institute of Geology and Mineralogy, Siberian Branch of the Russian Academy of Sciences, Novosibirsk,
[2] Novosibirsk State University, Novosibirsk
(*novoselovid@igm.nsc.ru*)

Abstract. CO_2 and CO_2-H_2O fluids are potential metasomatic agents in Earth's mantle. Interaction of garnet group minerals, as an integral part of mantle lithology, with these fluids seems to be possible. Experimental modeling of lherzolitic and eclogitic garnets carbonation in CO_2 and CO_2-H_2O fluids was carried out on the BARS equipment (6.3 GPa, 950-1250 °C, 60-100 h). During the interaction of garnets with CO_2 and CO_2-H_2O fluids magnesium and calcium are extracted from garnets while Mg-carbonate, kyanite, coesite and silicate-carbonate melts are formed. It was demonstrated that the carbonation of lherzolitic and eclogitic garnets under upper mantle PT-parameters is fundamentally possible and leads to the decrease of pyrope and grossular components in garnets and to the formation of carbonate and/or silicate-carbonate melt as well as kyanite and coesite. Obtained results allow considering aforementioned changes in garnets composition as indicators of mantle CO_2-based metasomatism.

Keywords: *garnet, lithospheric mantle, mantle metasomatism, CO_2-fluids, carbonate, high-pressure experiment.*

Mantle metasomatism is currently actively studied. It is strongly connected with fluid regime of subduction zones and of the mantle in general, with mantle mineral forming processes and with evolution of mantle rocks. Determination of how mineral assemblages and chemical compositions of individual phases change during metasomatic process is of great interest for mantle petrology. The most possible metasomatic agents in Earth's mantle are

CO_2 and CO_2-H_2O fluids. There are evidences of their presence in mantle, such as inclusions in diamonds containing great amounts of CO_2 (Schrauder and Navon, 1993). In previous works experimental modeling of carbonation and decarbonation reactions in silicate-carbonate systems was carried out and corresponding lines in PT-field were established. Decarbonation reactions resulting in diopside, forsterite, enstatite (Wyllie et al., 1983; Luth, 1995; Koziol, Newton, 1998; Pal'yanov et al., 2005) and garnets (Knoche et al., 1999; Pal'yanov et al., 2005; Bataleva et al., 2020) formation were experimentally modeled. Nevertheless, carbonation of minerals with complex stoichiometry is still unexplored. The main objective of this study is experimental modeling of mantle (eclogitic and lherzolitic) garnets carbonation in CO_2 and CO_2-H_2O fluids under lithospheric mantle PT-parameters.

Experiments were carried out on the multi-anvil high-pressure equipment of "split-sphere" type (BARS) at pressure of 6.3 GPa, temperatures of 950-1250 °C (with a 100 °C step) for 60-100 hours. Garnets from eclogite UD-45-02 (Kolesnichenko et al., 2018) and garnet lherzolite UD-11-04 (Shatsky et al., 2020; Kolesnichenko et al., 2017) xenoliths from Udachnaya pipe with compositions $(Mg_{2,01}Fe_{0,63}Ca_{0,44}Mn_{0,02}(Al_{1,87}Cr_{0,03}Ti_{0,02})[SiO_4]_3$ and $(Mg_{2,19}Fe_{0,47}Ca_{0,45})(Al_{1,49}Cr_{0,38}Ti_{0,04})[SiO_4]_3$ respectively, were taken as starting materials. Oxalic acid and silver oxalate were used as fluid sources. At experimental PT-parameters these reagents decompose according to the schemes:

$$Ag_2C_2O_4 = 2Ag^0 + 2CO_2 \quad (1)$$

$$2H_2C_2O_4 = 2H_2O + C^0 + 3CO_2 \quad (2)$$

Experiments were carried out in four systems: Grt_{EC}-CO_2, Grt_{LZ}-CO_2, Grt_{EC}-CO_2-H_2O и Grt_{LZ}-CO_2-H_2O (table 1) (Grt_{LZ} – lherzolitic garnet, Grt_{EC} – eclogitic garnet).

Table 1. Masses of starting reagents for experiments in systems garnet-CO_2 and garnet-CO_2-H_2O.

System	Mass, mg			
	Eclogitic garnet	Lherzolitic garnet	Silver oxalate	Oxalic acid
Grt_{EC}-CO_2	21.6	-	15.25	-
Grt_{LZ}-CO_2	-	21.75	15.25	-
Grt_{EC}-CO_2-H_2O	21.6	-	-	4.5
Grt_{LZ}-CO_2-H_2O	-	21.75	-	4.5

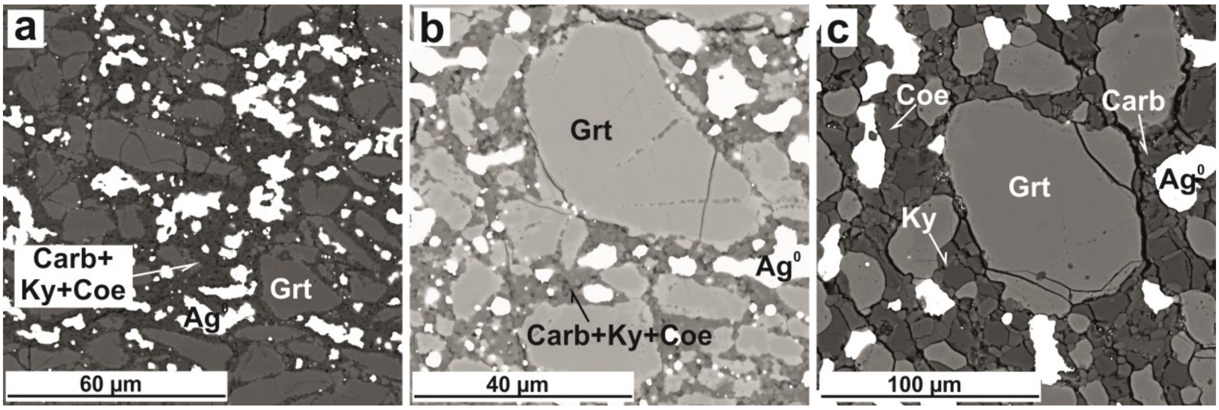

Figure 1. SEM images of samples from experiments in system Grt_{EC}-CO_2 at P = 6.3 GPa and T = 950 °C, t = 100 hours (a), 1150 °C, t = 80 hours (b), 1250 °C, t = 60 hours (c). Grt – garnet, Carb – magnesian carbonate, Ky – kyanite, Coe – coesite, Ag^0 – silver.

Starting materials were loaded in platinum ampules with inner graphite capsules. Platinum allows effectively containing the fluid and melts during the experiments, while graphite isolates starting materials from the platinum and prevents iron extraction from the sample. In experiments with dry CO_2 fluid hematite redox buffer was used in a high-pressure cell construction for averting hydrogen diffusion into the ampules.

In Grt_{EC}-CO_2 system recrystallized garnet, carbonate, coesite and kyanite were formed (fig. 1). It was determined that newly formed carbonate is significantly magnesian, and recrystallized garnet gets enriched in calcium and depleted in magnesium relatively to the initial.

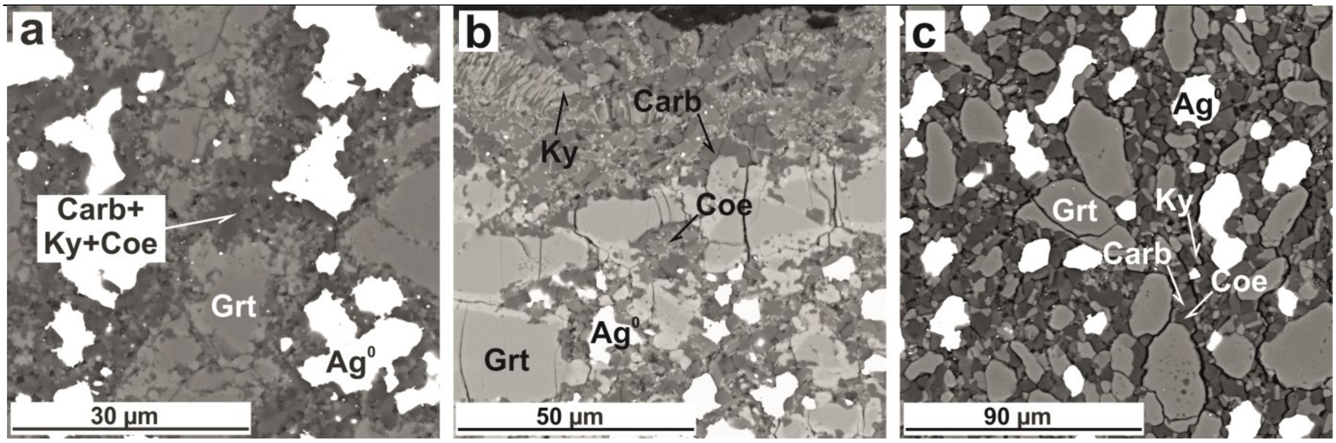

Figure 2. SEM images of samples from experiments in system Grt_{LZ}-CO_2 at P = 6.3 GPa and T = 950 °C, t = 100 hours (a), 1150 °C, t = 80 hours (b), 1250 °C, t = 60 hours (c). Grt – garnet, Carb – magnesian carbonate, Ky – kyanite, Coe – coesite, Ag^0 – silver.

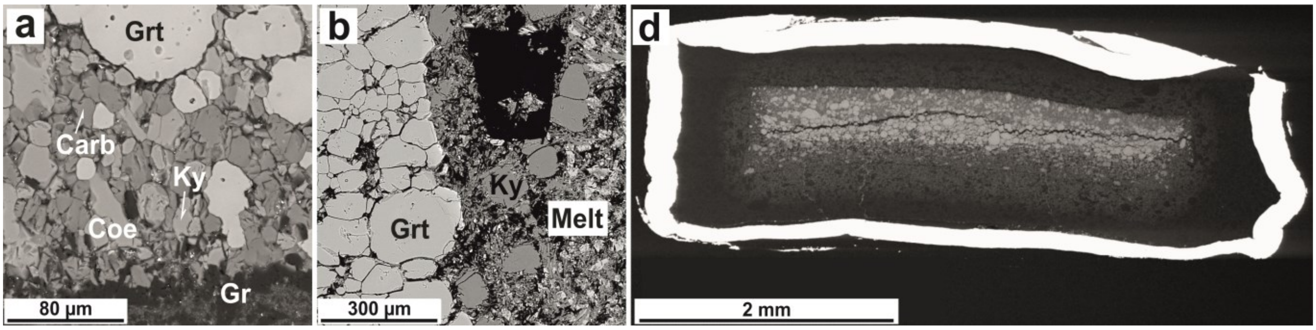

Figure 3. SEM images of samples from experiments in system Grt_{EC}-CO_2-H_2O at P = 6.3 GPa and T = 1050 °C, t = 100 hours (a, c), 1250 °C, t = 60 hours (b). Grt – garnet, Carb – magnesian carbonate, Ky – kyanite, Coe – coesite, Melt – silicate-carbonate melt.

In Grt_{LZ}-CO_2 system formation of recrystallized garnet, carbonate, coesite and kyanite was established (fig. 2). Chemical analyses of obtained phases showed that recrystallized garnet is enriching in calcium and depleting in magnesium relatively to the initial while newly formed carbonate has predominantly magnesian composition.

Sample obtained in Grt_{EC}-CO_2-H_2O system at 6.3 GPa and 950 °C is composed out of recrystallized garnet, carbonate, coesite and kyanite. At 1050-1150 °C silicate-carbonate melt coexisting with magnesian carbonate appears. At 1250 °C formation of silicate-carbonate melt was registered as well, but liquidus carbonate wasn't found (fig. 3). In experiments without melting pyrope content in garnet is decreasing while grossular content is increasing; carbonate in these experiments is highly magnesian. In experiments with partial melting grossular content decrease and pyrope content increase in garnet is observed, while silicate-carbonate melt is getting enriched in calcium.

In Grt_{LZ}-CO_2-H_2O system at 6,3 ГПа and 950 °C assemblage of recrystallized garnet, coesite, kyanite and carbonate was obtained. At 1050-1150 °C silicate-carbonate melt coexisting with magnesian carbonate was formed. At 1250 °C sample is composed out of recrystallized garnet, chromium bearing kyanite and silicate-carbonate melt. The main trend of recrystallized garnet composition changes is generally similar to that in Grt_{EC}-CO_2-H_2O system. However, it should be noted that in Grt_{LZ}-CO_2-H_2O system kyanite is significantly chromium-saturated (up to 0.6 formula units). Cr/(Cr+Al) ratio is higher in kyanite, than in garnet, and increases with temperature increase.

Hereby, it was demonstrated that lherzolitic and eclogitic garnets recrystallize and get carbonated in fluid/melt at experimental PT-parameters according to two schemes:

$$\mathrm{Grt} + 3CO_2 = 3\mathrm{Carb} + \mathrm{Ky} + 2\mathrm{Coe} \qquad (3)$$

$$\mathrm{Grt} + CO_2 + H_2O = \mathrm{Ky} + \mathrm{Melt} \qquad (4)$$

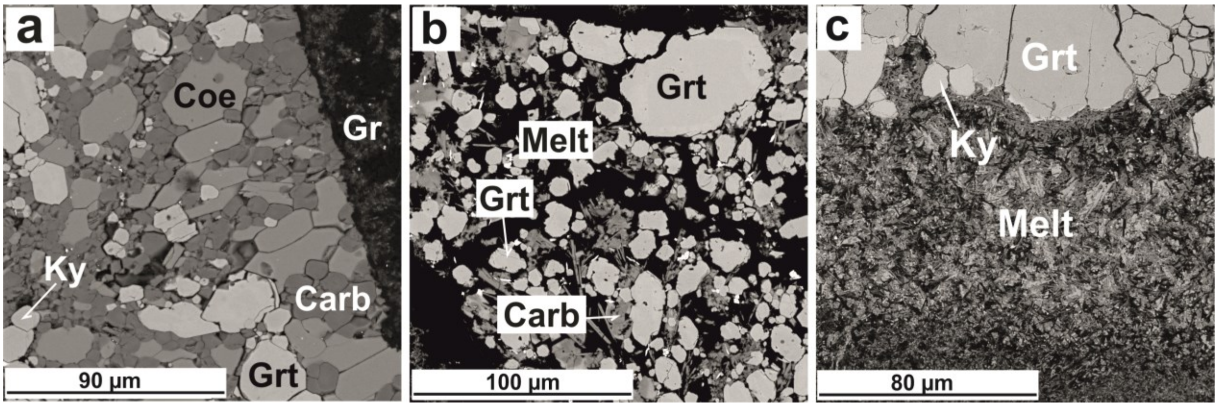

Figure 4. SEM images of samples from experiments in system Grt_{LZ}-CO_2-H_2O at P = 6.3 GPa and T = 1150 °C, t = 80 hours (a, b), 1250 °C, t = 60 hours (c). Grt – garnet, Carb – magnesian carbonate, Ky – kyanite, Coe – coesite, Melt – silicate-carbonate melt.

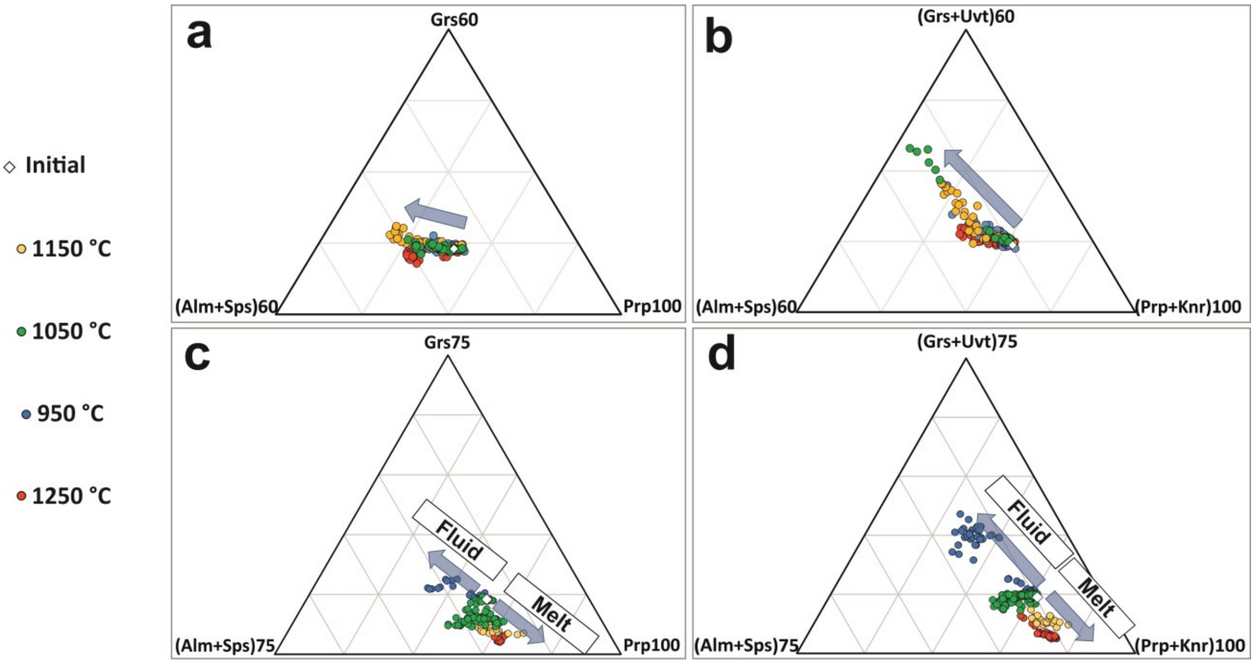

Figure 5. Compositions of garnets obtained in Grt_{EC}-CO_2 (a), Grt_{LZ}-CO_2 (b), Grt_{EC}-CO_2-H_2O (c), and Grt_{LZ}-CO_2-H_2O (d) systems at 6.3 GPa and 950-1250 °C. Components: Alm – almandine, Sps – spessartine, Grs – grossular, Prp – pyrope, Uvt – uvarovite, Knr – knorringite.

Scheme (3) corresponds to carbonation without melting, scheme (4) corresponds to carbonation with partial melting achieved. According to the scheme (3) recrystallized garnet enriches in calcium and depletes in magnesium, according to scheme (4) garnet depletes in calcium (fig. 5). It is important to mention behavior of chromium: in Grt_{LZ}-CO_2-H_2O system Cr/(Cr+Al) ratio is higher in kyanite than in garnet and rises up with temperature increase. This regularity can be explained through coherency of chromium in studied system.

Obtained data can be interpreted towards the mantle rocks as follows:

- In mantle areas with thermal flow insufficient for partial melting of carbonated eclogites and lherzolites carbonation will lead to decrease of garnet magnesian number and formation of magnesian carbonates;
- In mantle areas with thermal flow sufficient for partial melting of carbonated eclogites and lherzolites carbonation will result in decrease of garnet calcium number;
- In lherzolitic systems processes of CO_2-H_2O-based metasomatism will be accompanied by decrease of knorringite component content in garnet, while components of chromium-bearing kyanite will, most probably, dissolve in clinopyroxenes.

Work is done on state assignment of IGM SB RAS, and founded by Ministry of Science and Higher Education of the Russian Federation.

References

Bataleva Yu.V., Novoselov I.D., Kruk A.N., Furman O.V., Reutsky V.N., Palyanov Yu.N. Experimental modeling of decarbonation reactions resulting in Mg,Fe-garnets and CO_2 fluid at the mantle P-T parameters // Russian Geology and Geophysics, 2020, vol. 61 (5-6), pp. 650-662.

Knoche R., Sweeney R.J., Luth R.W. Carbonation and decarbonation of eclogites: the role of garnet // Contributions to Mineralogy and Petrology, 1999, vol. 135(4), pp. 332–339.

Kolesnichenko M.V., Zedgenizov D.A., Litasov K.D., Safonova I.Y., Ragozin A.L. Heterogeneous distribution of water in the mantle beneath the central Siberian Craton: Implications from the Udachnaya Kimberlite Pipe // Gondwana Research, 2017, vol. 47, pp. 249–266.

Kolesnichenko M.V., Zedgenizov D.A., Ragozin A.L., Litasov K.D., Shatsky V.S. The role of eclogites in the redistribution of water in the subcontinental mantle of the Siberian craton: results of determination of the water content in minerals from the Udachnaya pipe eclogites // Russian Geology and Geophysics, 2018, vol. 59(7), pp. 763–779.

Koziol A.M., Newton RC. Experimental determination of the reaction; magnesite + enstatite = forsterite + CO_2 in the ranges 6-25 kbar and 700-1100 degrees C // American Mineralogist, 1998, vol. 83(3-4), pp. 213–219.

Luth RW. Experimental determination of the reaction dolomite + 2coesite = diopside + $2CO_2$ to 6 GPa // Contributions to Mineralogy and Petrology, 1995, vol. 122(1-2), pp. 152–158.

Palyanov Y.N., Sokol A.G., Tomilenko A.A., Sobolev N.V. Conditions of diamond formation through carbonate-silicate interaction // European Journal of Mineralogy, 2005, vol. 17(2), pp. 207–214.

Schrauder, M., Navon, O. Solid carbon dioxide in a natural diamond // Nature, 1993, vol. 365(6441), pp. 42–44.

Shatsky V.S., Ragozin A.L., Kozmenko O.A., Denisenko A.A. Geochemical evidence for participation of the subducted crust in the process of transformation of the subcontinental mantle in the Yakutian diamondiferious province // Doklady Earth Sciences, 2020, vol. 493, pp. 513-516.

Wyllie P.J., Huang W.-L., Otto J., Byrnes A.P. Carbonation of peridotites and decarbonation of siliceous dolomites represented in the system CaO-MgO-SiO_2-CO_2 to 30 kbar // Tectonophysics, 1983, vol. 100(1-3), pp. 359–388.

Shchekina T.I.[1], Zinovieva N.G.[1], Rusak A.A.[2], Khvostikov V.A.[3], Alferyeva Ya.O.[1], Kotelnikov A.R.[4] Behavior of rare-earth elements during crystallization of model granite system with water and fluorine UDC 552.11

1- Lomonosov Moscow State University, Department of Geology, Moscow, [2](GEOKHI RAS), Moscow, [3](IPTM RAS), [4](IEM RAS) (t-shchekina@mail.ru; nzinov@mail.ru; aleks7975@yandex.ru; khvos@ipmt-hpm.ac.ru; yanaalf@yandex.ru; kotelnik@iem.ac.ru)

Abstract. The behavior of rare-earth elements (REE), Y, Sc in a model granite system Si-Al-Na-K-Li-F-O-H with a limiting fluorine content at temperatures from 800 to 500 °C, a pressure of 1 kbar has been studied. Starting from 800 °C, when a region of liquid immiscibility appears in the system, all rare-earth elements are predominantly concentrated in the LF saline aluminofluoride melt in comparison with the silicate one. The partition coefficients between salt and aluminosilicate melts are much higher than KD_{REE} (LF/L) >> 1. Rare-earth elements do not form their own phases in the silicate melt. With a decrease in temperature down to 500 °C, REEs continue to accumulate in the residual molten salt globules filling the interstitiums between the K-Na- aluminofluorides crystallizing in them. At temperature below 500 °C, the salt melt crystallizes, and REE, Y, Sc form fluoride compounds of the LnF_3 type (analogue of fluocerite CeF_3) or $(Na,K)_3LnF_6$ (analogue of gagarinite $NaCaYF_6$). Only scandium from the considered group of elements shows a tendency to enter the structures of other phases crystallizing in the system, partially replacing Al in cryolite $(Na, K)_3(Al, Sc)F_6$ and Li-mica, similar to polylithionite $KLi_2(Al, Sc)Si_4O_{10}(F,OH)_2$. At 800 and 750 °C, a positive correlation is observed between the separation coefficients of REE, Y, Sc, and Li. The significant accumulation of REE in residual salt melts rich in volatile components (H_2O and F) indicates a possible mechanism for the concentration of REE, Y, and Sc in granite massifs at the last stages of their differentiation and in pegmatites.

Keywords: *partition coefficient, rare-earth elements, lithium, silicate and aluminofluoride salt melt.*

The aim of the work was to study the phase relations and behavior of rare-earth elements with a decrease in temperature from 800 to 500 °C and a pressure of 1 kbar in a model high-fluoride granite system Si-Al-Na-K-Li-F-O-H. It was previously shown (Gramenitskiy et al., 2005; Shchekina et al., 2020; 2021) that, starting from 800 °C, a region of liquid immiscibility appears in the system, and all rare-earth elements are predominantly concentrated in the LF salt aluminofluoride melt with high partition coefficients >> 1 in comparison with silicate one. As a rule, they do not form their own phases. Only occasionally they are precipitated in the form of a thin rim of fluorides at the interface between the salt and silicate quenched melts.

In the study, the task was set to find out how REEs will behave when cooling the system under conditions of equilibrium crystallization of minerals from both melts and what will be their distribution between coexisting melts and minerals. It was especially important to understand how the salt melt will crystallize, and which natural phases will form the rare-earth elements.

Technique and methodology. The experiments were carried out on a high gas pressure unit with internal heating at a temperature of 500-800 °C and a pressure of 1 kbar. The temperature measurement error was ± 5 °C, and the pressure measurement error was ± 10 bar. Oxygen volatility in the experiments corresponded to that created by the NNO buffer. The duration of the experiments was 7 days. Platinum ampoules with a diameter of 3 mm were used as containers for the substance of the experiments.

Experiments at 500-600 °C were carried out in two stages, using the "top" approach to equilibrium. The ampoules with the substance were heated to 800 °C at a pressure of 1 kbar, kept for 3 days, and slowly cooled to a predetermined temperature for 8 hours. Then they were kept for 3 days at 600, 550, 500 °C and quenched. The quenching rate on the high pressure unit was 150-200 degrees per minute.

The initial charge was a silicate-salt mixture of reagents. Silicate part corresponded to the composition of the aluminosilicate melt, close to the granite eutectic saturated with water. The salt part of the charge was a composition corresponding to the stoichiometry of the compound $(Na, K, Li)_3AlF_6$ in an amount sufficient to saturate the aluminosilicate melt with it and generation an isolated aluminofluoride phase (Table 1).

Table 1. The initial composition of the silicate-salt mixture (100%) - the reference composition A-40/11 for all series of experiments (at.%).

Si	Al	Na	K	Li	F	O	Sum
17.24	6.92	5.07	3.84	4.46	21.82	40.65	100

The water content in the system was about 10-15 wt. %. The following reagents and compounds were used as starting materials for preparing the charge: dried gel SiO_2, NaF, LiF, AlF_3, Al_2O_3, K_2SiF_6. Rare-earth elements La, Ce, Pr, Nd, Sm, Eu, Gd, Tb, Dy, Ho, Er, Tm, Yb, Lu, as well as Y and Sc were introduced into the system in the form of oxides in an amount of 0.5-2 wt% element.

The study of the phase relations and the chemical composition of the solid products of the experiments was carried out by the methods of electron microscopy and electron probe microanalysis in the laboratory of local methods for the study of matter of the Department of Petrology and Volcanology of the Geological Faculty of Moscow State University.

Electronic images are obtained in reflected electron mode (BSE). The analysis of the main elements and fluorine in phases was carried out using a Jeol JSM-6480LV scanning electron microscope (Japan) with an energy-dispersive Oxford X-Max^N and INCA Wave-500 crystal diffraction spectroscopes (Oxford Instrument Ltd., UK). Shooting conditions: voltage 20 kV, current 0.7 nA. The accuracy of the estimation of the main elements in the composition of the synthesized phases was 2–5 rel.%. The instrumental error in the measurement of fluorine was ± 1% of the element concentration.

In a number of samples, the main and rare-earth elements in silicate glasses were studied using a *Superprobe JXA-8230 electron probe microanalyzer (Japan)*. To prevent glass destruction, the analyzes were performed in the defocused beam mode (up to 10 µm) at an accelerating voltage of 10 kV and a current strength of 10 nA. At the time of measuring the peak and background intensities (30/15 sec), the dispersion of the measurements of Si, Al, and O was 0.8 rel.%, K was 1.5 rel.%, Na was 2 rel.%, F was 2 rel. %. Rare-earth elements were analyzed at an accelerating voltage of 20 kV and a current of 30 nA. The accumulation time for various rare-earth elements was selected so that their detection limit did not exceed 0.01%.

The methods of inductively coupled plasma mass spectrometry and laser ablation (La-ICP MS) were used to determine Li and REE, Y, Sc, as well as Si, Al, Na, K at the Analytical Certification Testing Center of the Institute for Problems of Microelectronics Technology and High Purity Materials of the Russian Academy of Sciences (ASIC IPTM RAS).

The measurements were carried out on an X Series II inductively coupled plasma quadrupole mass spectrometer (Thermo Scientific, USA) with an UP266 MACRO laser ablation attachment (New Wave Research, USA) with the following operating parameters: mass spectrometer - RF generator output power 1200 W, the flow rate of the plasma-forming argon flow is 13 l/min, the auxiliary flow is –0.90 l/min, the flow rate of the carrier gas He is 0.6 l/min followed by mixing with Ar 0.6 l/min, the resolution is 0.4 and 0.8 M; attachment for laser ablation - laser wavelength 266 nm, pulse repetition rate 10 Hz, pulse energy 3 mJ, pulse duration 4 ns, crater diameter 60 µm. The time of one measurement was 10 s. If the sample size allowed, the laser beam was scanned over the surface at a speed of 20 µm/s; otherwise, the “in-point” ablation mode was used. Up to 5 measurements were carried out on each sample (depending on the sample size) and the results were averaged. The analytical error of most elements was less than 10% of the measured value. External calibration was performed using NIST SRM-610-616 standard silicate glass samples. Silicon was used as an internal standard. In addition, an additional correction of the matrix was carried out, taking into account that the elements of the base of the glass phase are in it in the form of oxides, and the salt phase in the form of fluorides.

Results. The phase composition of the products of experiments carried out at 800, 750 °C is presented (fig.1a, b) by quenched aluminosilicate glass, which constitutes the matrix of the samples, and salt melt in the form of an aggregate of small quenching crystals of aluminofluorides Na, K, Li of gray color (image in the mode backscattered electrons BSE) and light gray fluorides (in BSE) REE, Y, and Sc (Shchekina et al., 2020, 2021). When the temperature drops to 600 °C, quartz and sodium and sodium-potassium aluminofluorides begin to crystallize from the aluminosilicate melt. The average composition of aluminosilicate glass (Table

2) is characterized by an agpaite coefficient close to unity (1.02 ± 0.07). It is enriched in potassium in relation to sodium by 2.7 times (in at. %), it contains hundredths of Ca percent.

The salt melt also begins to crystallize at temperatures below 750 °C. At 700 °C, large precipitates of KNa-aluminofluorides of cryolite stoichiometry appear in some salt globules. At 600 °C, they occupy a larger (about 3/4) space of globules, but a salt melt, sharply enriched in rare earth elements, remains between them (fig. 1 c, d). Borders of Li-mica and polylithionite crystallize along the boundary between the globules and glass. It contains Sc, partially replacing Al.

At 500 °C, the crystallization of silicate and salt melts continues. The phase relationships remain the same as at 600 °C. The compositions of the melts in terms of the main components are close to those at 600 °C. For Si, Al, the separation coefficients KD (LF / L) may hardly change, but they increase for Li and slightly decrease for Na and K. Significant changes occur in the behavior of rare-earth elements as the temperature decreases from 750 to 500 °C. The residual salt melt is enriched in REE, Y, and Sc, which is clearly seen from both electronic photographs (fig.1c, d) and high (up to the first wt. %) REE contents. At the same time, $KD_{REE}^{(LF / L)}$ in experiments at 600 - 500 °C become lower than at 750 °C (fig. 2). This occurs as a result of the relatively greater accumulation of REE in the silicate melt at 600 °C and 500 °C, which decreases the KD as compared to the experiments at 750 °C. In fig. 2 shows a large scatter of data at 600 °C and 500 °C. To obtain more firm REE data, additional determinations of the composition of the residual molten salt are required.

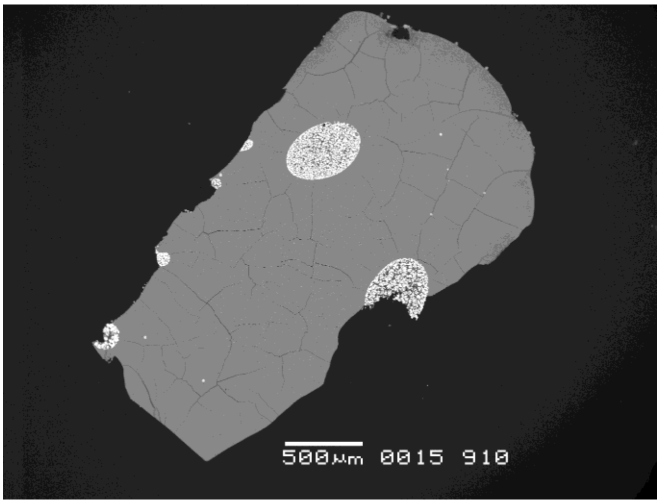

Fig.1a. Large globules of salt melt in silicate glass at 750 °C.

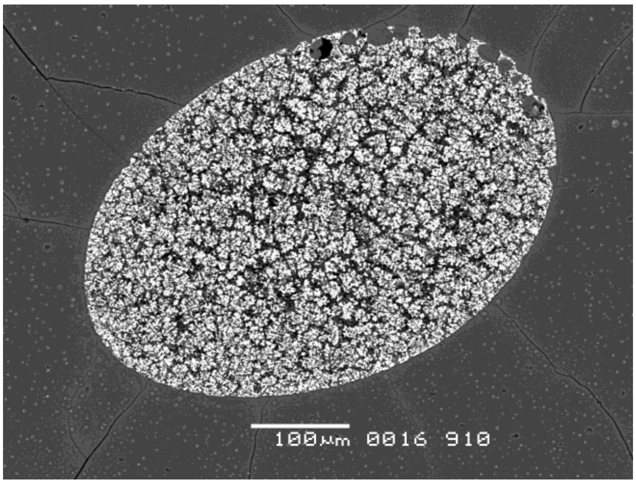

Fig.1b. Uniformly distributed quenching phases of Na, K, Li aluminofluorides and REE, Y, Sc fluorides at 750 °C.

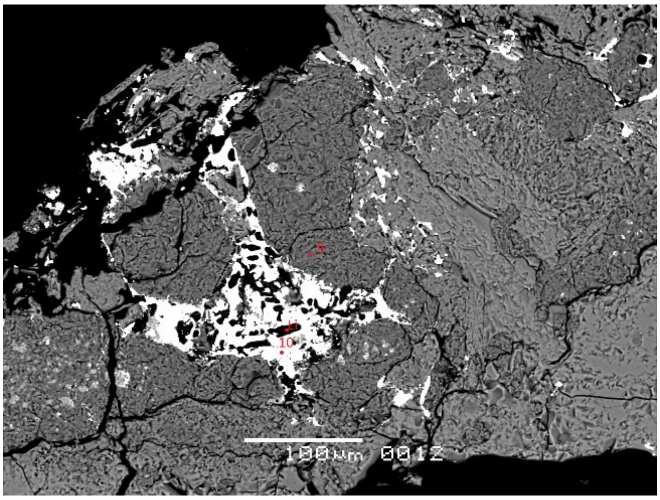

Fig. 1c. Fragment of a salt globule composed of crystals of Na-K aluminofluoride (gray in BSE) and quenched residual melt between them at 600 °C.

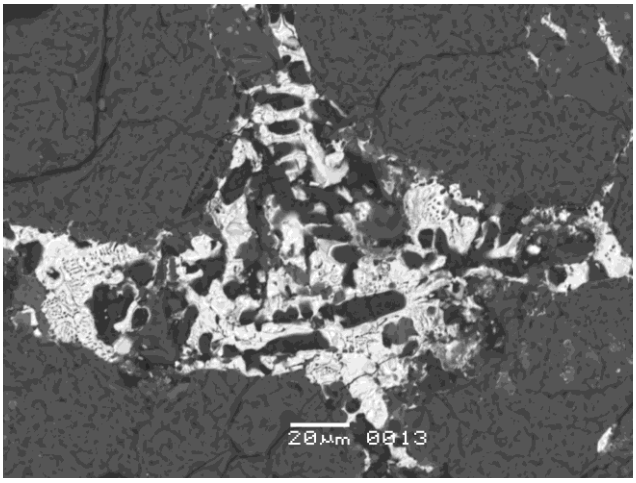

Detail fig. 1c. Quenched residual melt consisting of light gray quenched REE fluorides, dark gray precipitates of LiF, and Na and K aluminofluorides at 600 °C.

Table 2. The composition of aluminosilicate glass L (X is the average value, S is the standard deviation) and the ratio of the main components at 600 °C, 1 kbar.

Element content	Phase	Si	Al	Na	K	Mg	Ca	F	O	Total
X 869-874 L, mas.%	L	29.67	7.05	1.66	7.41	0.01	0.02	6.98	45.58	98.38
S 869-874 L	L	1.07	0.42	0.29	0.45	0.01	0.01	0.92	0.56	
X 869-874 L, at.%	L	22.50	5.52	1.51	4.14	0.01	0.01	7.59	58.71	100.00
S 869-974 L	L	1.60	0.26	0.25	0.48	0.01	0.01	1.04	1.59	

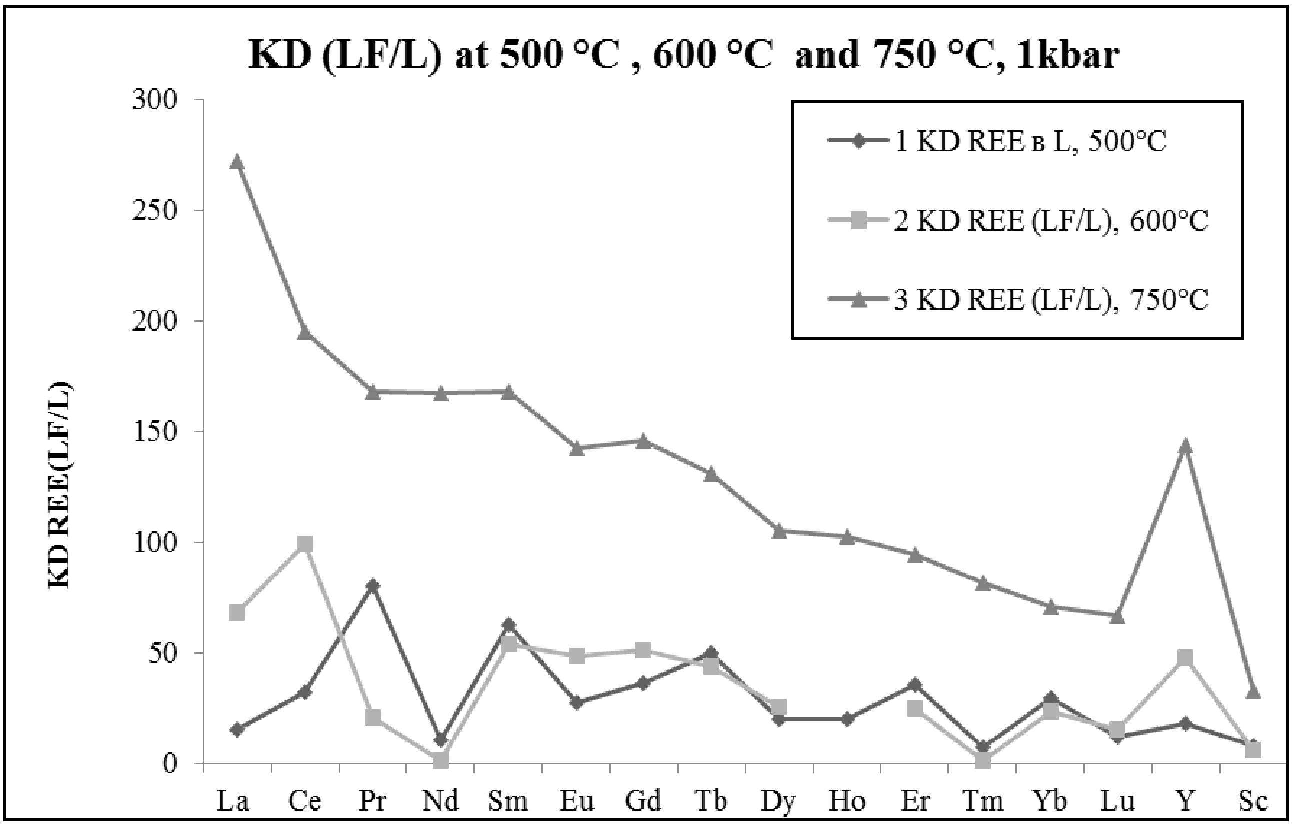

Fig. 2. Data on the distribution coefficients of REE between the salt and aluminosilicate melt at temperatures of 500, 600 and 750 °C.

In addition to studying the composition of silicate and salt melts, the REE phases were analyzed within the salt globules, represented by small crystals with a size of 2-3 µm. Among them, phases similar to simple rare-earth fluorides of the LnF_3 type were found: DyF_3, $(Y_{0.85}La_{0.15})F_{2.3}$, etc., as well as alkali fluorides similar to $NaLnF_4$: $(Na_{0.04}K_{0.18})_{0.61}(Y_{0.85}La_{0.15})F_{3.9}$ and $(Na_{0.23}K_{0.29})_{0.55}(Nd_{0.14}Tm_{0.86})F_{3.9}$. Compounds of this type with different ions of the REE group (called up-conversion nanoparticles) are used as biomarkers. Some of them are soluble in water and can, in the form of fluoride complex compounds, pass into hydrothermal solutions and accumulate already in the postmagmatic stage.

Conclusion

1. It is shown that rare-earth elements during cooling and crystallization of high-fluoride, water-saturated granite melt continue to concentrate up to 500 °C in the composition of the residual salt melt.
2. With decreasing temperature, a partial redistribution of REE between salt and silicate melts occurs, as a result of which the partition coefficients between salt and silicate melts $KD_{REE}^{(LF/L)}$ decrease.

References

Gramenitsky E.N., Schekina T.I., Devyatova V.N. Phase relations in fluorine-containing granite and nepheline-syenite systems and distribution of elements between phases. M. : GEOS. 2005. 186 p.

Shchekina T.I., Rusak A.A., Alferyeva Ya.O., Gramenitskiy E.N., Kotelnikov A.R., Zinovyeva N.G., Bychkov A.Yu., Bychkova Ya.V., Khvostikov V..A. Distribution of REE, Y, Sc and Li between aluminosilicate and aluminofluoride melts in a model granite system depending on pressure and water content // Geokhimiya, Nauka (Moscow), 2020, vol. 65, № 4, pp. 343-361.

Shchekina T.I., Rusak A.A., Alferyeva Ya.O., Gramenitskiy E.N., Khvostikov V.A., Kotelnikov A.R., Bychkov A.Yu., Zinovieva N.G. Behavior of lithium in the liquidus part of a high-fluoride granite system at a pressure of 10 to 50 MPa // Moscow University Bulletin. Series 4: Geology, Moscow Publishing House. University (M.), 2021. № 3, pp. 76-88.